Universidade do Algarve

Faculdade de Ciências e Tecnologia

Spectral Analysis of Coronary Bypass Doppler Blood Flow Signals

Behrooz Zabihian

Masters in Electronics and Telecommunications Engineering

March 2011

Universidade do Algarve

Faculdade de Ciências e Tecnologia

Spectral Analysis of Coronary Bypass Doppler Blood Flow Signals

Behrooz Zabihian

Supervisor

Prof[a]. Doutora M. Graça Ruano

Masters in Electronics and Telecommunications Engineering

March 2011

Abstract

The pulsed Doppler ultrasound (DU) is one of the important tools in the study of vessel diseases and the investigation of flow conditions. Due to its non-invasive nature, it has been increasingly used in medicine in the last few decades. Accurate estimation of DU spectral center frequency and bandwidth parameters are extremely important for blood flow diagnostic purposes. Under real-time data acquisition conditions the DU signal is generally corrupted with different types of noise. In these situations the identification of signal components solely belonging to the blood flow signal is a difficult task.

This thesis was aimed to study spectral techniques to enhance spectral parameter estimation, in particular the center frequency. Spectral estimates were obtained using the Short Time Fourier Transform (STFT) and Continuous Wavelet Transform (CWT). STFT was applied to short duration data segments, respecting signals' stationary properties. Two CWT functions have been studied: varying bandwidth filter and fixed bandwidth filter. Since different filter bandwidth values yield different results, bandwidths for fixed bandwidth filter were investigate and the most proper one has been used on the performance comparative studies. To enhance the blood flow signal content of noise-embedded clinical Doppler signals, a STFT-based technique was proposed to reduce the signals' noise components.

Quantitative evaluation of the spectral methods was primarily performed on simulated signals with deterministic center frequency and bandwidth. Different signal to noise ratio signals were simulated. It has been observed that STFT spectral center frequency and bandwidth estimators were less biased than the CWT ones, although the last ones were less sensitive to the center frequency variations.

Applying the proposed noise cancellation technique to simulated signals reduces the spectral estimators' errors. As an example, a typical noisy signal with $10dbSNR$, a reduction of 88% and 97% was obtained on the RMS bias of the estimation of the center frequency and bandwidth estimators respectively.

Keywords: Doppler spectrum, STFT, wavelets, noise cancellation, ultrasound, blood flow signal.

Resumo

O ultra-som Doppler pulsado é um importante instrumento utilizado no estudo de doenças vasculares e na investigação das condições de fluxo sanguíneo. Devido á sua natureza não invasiva, tem sido crescentemente utilizado nas últimas décadas. A estimativa precisa de parâmetros como sejam a frequência central e a largura da banda do espectro Doppler de ultra-som são extremamente importantes no diagnóstico de anomalias do fluxo sanguíneo. Nestas situações, a identificação de componentes de sinal pertencendo somente ao sinal de fluxo sanguíneo é uma tarefa difícil.

Pretendia estudar-se nesta tese técnicas que melhorassem a qualidade da estimativa espectral, particularmente da frequência central. Foram obtidas estimativas do espectro usando a Transformada de Fourier de Tempo Reduzido (STFT) e a Transformada Contínua de Wavelet (CWT). A STFT foi aplicada a segmentos do sinal de curta duração, respeitando as suas características de estacionaridade. Estudaram-se duas funções da CWT: O filtro de largura da banda variada e a filtro de largura da banda fixa. Uma vez que diferentes larguras de banda do filtro produzem resultados diferentes, foram investigados possíveis valores para a largura da banda do filtro de largura da banda fixa, tendo-se escolhido o valor mais apropriado para utilização nos estudos comparativos de desempenho. Para melhorar o conteúdo do sinal sanguíneo em sinais clínicos Doppler ruidosos, foi proposta uma metodologia de redução de ruídos das componentes do sinal.

A avaliação quantitativa dos resultados foi inicialmente feita com base em sinais simulados de frequência central e largura de banda determinísticos. Diferentes níveis de sinal-ruído foram simulados. Observou-se que os estimadores frequência central e largura de banda eram menos enviesados quando se utilizava a STFT do que utilizando a CTW; contudo, esta última produzia estimativas menos sensíveis á forma de onda de frequência central.

Os erros da estimação espectral reduzem quando a técnica de cancelamento de ruído proposta é aplicada. A título de exemplo, aplicando-a a um sinal tipicamente ruidoso com $10dB$ de SNR, as estimativas da frequência central e da largura de banda reduzem o viés rms de 88% e 97% respectivamente.

Palavras-chave: Espectro Doppler, STFT, wavelets, cancelamento de ruído, ultra-som, sinal de fluxo sanguíneo.

Contents

List of Figures

Chapter 1

Introduction

1.1 Motivation

The upward trend of the development of science and technology in the twentieth century, profoundly encompasses the life style of human kind. The dependency of our lives on the new discoveries in science and technology is substantial. These discoveries enrich the quality of life and improves our daily activities. Investments in science and medicine lead to achievements all around the globe. These achievements help to save lives of thousands of people, cure numerous diseases and amend lives of millions of people. Perhaps it wont be too far from the reality if we consider any new achievement a simple aid to either save lives or improve quality of life.

In this context, engineering sciences indeed carry out a major role in the development of instruments used in medicine. Medicine and engineering endorsing each other, help us to have better and improved lives. Thank to the achievements in medicine, life expectancy is getting higher, more diseases become curable and lives of more people become better and improved.

Any progress in engineering of devices, tools and the technology used in medicine, in fact would serve our lives. By nature, upon arrival to any new stage, man kind demands to get to a higher one. In engineering, any single invention led

to a faster, more powerful and more precise invention. Moreover to the desire of the man kind, the society necessitates and requests the progressive development of tools. In medicine, for instance, during 1970s the efficacy of carotid endarterectomy was debated. At the time, carotid endarterectomy was a well established and recognized procedure to deal with stenotic vessels. However, based on the reports of high rate of mortality after surgery, The steadily increasing number of carotid endarterectomy started to decline. The international medical society demanded establishment of particular criteria to evaluate effectiveness of carotid endarterectomy on patients with specific stenotic degree. Doppler ultrasound devices were among the best noninvasive methods to estimate stenotic degree on vessels.

The first report of application of Doppler ultrasound in medical diagnosis dates back to 1956. Satomura and his group from Osaka University, Japan, reported the detection of heart wall motion using Doppler Ultrasound. Merely two decades after this report, Doppler ultrasound methodology progressed massively. In 1978, color Doppler imaging system using continuous wave signals was introduced. In this system, regions with increased flow velocity were distinguished by color coding from normal flow velocity regions. Eventually by the early 1990's in Europe and North America, the official criteria for carotid endarterectomy procedure based on the stenotic degree on vessels were established. The topic is yet to be investigated and still there are many aspects of this methodology to be researched. The particular motivation of the current thesis is to study techniques to improve spectral estimation of Doppler ultrasound blood flow signals.

1.2 Proposed Goals

This work was aimed to study the application of spectral estimator methods on the estimation of Doppler ultrasound blood flow spectral mean frequencies. This main goal should be achieved by primarily investigating a method for reducing the noise content of the clinical signals. Then, more than one spectral estimator method should be tested aiming at the determination of spectral mean frequency (mean blood flow) curves for each cardiac cycle. To help on the spectral estima-

tion methods' understanding and characterization usage of simulated signals was suggested. In this sense, an existent computational program to simulate Doppler signals has been employed.

1.3 Thesis Outline

This thesis consists of five chapters. The first chapter is the introduction and includes the sections about motivation of the work, proposed goals and outline of the thesis. Second chapter is dedicated to the theoretical background. This chapter has two main sections. In the first section a historical overview of development of Doppler ultrasound concerning its medical application is presented. Section ends with the theoretical background of Doppler ultrasound signal simulator used in this study. This simulator is briefly described and its corresponding mathematical expressions are presented. In the second main section of this chapter, spectral estimators are being explained. In this part, Fourier based and Continuous Wavelet transformation are annotated. At the end of this chapter the expression to estimate the center frequency and the bandwidth are presented.

The third chapter is on the methods applied in this study. In this chapter, Short Time Fourier Transform (STFT) is described. A proposed technique to eliminate the noise based on STFT is thoroughly presented. The Continuous Wavelet Transform (CWT) is the other applied method. Presented are the used wavelet base in this study, fixed bandwidth filter and varying bandwidth filter.

The fourth chapter is devoted to the obtained results. The noise content of the clinical signals is being analyzed. Three different clinical signals are presented to exhibit the variation of magnitude of noise in different signals. Results of the STFT, CWT with fixed bandwidth filter and CWT with varying bandwidth filter are presented. Finally the results of application of these three methods for spectral estimation on the clinical signals are presented.

The fifth chapter offers the conclusions and the proposals of future work.

Chapter 2

Theoretical Background

2.1 Introduction

This chapter is devoted to the theoretical background of this work and has two parts. The first part concerns the Doppler ultrasound blood flow signals. Primarily a historical overview of Doppler ultrasound methodology and application of this methodology on blood flow signals is presented. The importance of application of Doppler ultrasound on carotid artery is briefly described. The simulator used in this study and reported in literature is introduced. Second part of this chapter deals with the spectral parameters. Two spectral estimation methods were used in this work: Short Time Fourier Transform and Continuous Wavelet Transform. Primarily, the need for the STFT is exemplified and it is showed why the Fourier Transform is inadequate in particular cases in digital signal processing; Then the CWT method and time-scale representation are introduced. Then the two transformation methods are compared. At last, the power waveform is formulated and the expressions to estimate the center frequency and the bandwidth are presented. The terms center frequency and mean frequency are used interchangeably in this thesis and both refer to the same concept.

2.2 Doppler Ultrasound Blood Flow Signals

Application of Doppler ultrasound is based on the idea of detecting the Doppler shift in the frequency of the ultrasound that is backscattered from a moving object. The stepping stone in Doppler ultrasound as a medical diagnosis tool is the work done by Shigeo Satomura at Osaka University, Japan [1]. Satomura and his associates published an article in 1956 and reported the Doppler ultrasound detection of heart wall motion using $3MHz$ ultrasound signals. Satomura and his associates studied three different applications to further develop Doppler methodology. One of these applications was flow in peripheral vessels. This research indicated that blood flow in peripheral arteries and veins could be detected transcutaneously. Another important outcome of this research was that the frequency of the reflected waves was proportional to the velocity of the blood flow. They had suggested the potential for using the methodology to study atherosclerotic arteries. Atherosclerosis is a vascular disease in which an artery wall thickens and causes stenotic lesions in arteries. Kanemasa Kato, another Japanese scholar along with his associates showed that Doppler signals were originating from moving red cells. They demonstrated that the frequency of these signals were related to the velocity and their output voltage related to the number of red cells. In 1965, Ziro Kaneko and his associates from Osaka University found that spectrum analysis provided the best means for analyzing Doppler signals.

The mainstream efforts of early Japanese investigators were endeavored to study the extracranial cerebral arteries. This work let to the demonstration of the difference between Doppler signal from carotid arteries obtained from patients with atherosclerosis and healthy subjects [1]. Meanwhile, along with Japanese investigators, American scholars were working on ultrasound in late 50's and early 60's. Dean Franklin from University of Washington by developing a transit-time recorder was employing ultrasound to study cardiovascular dynamics. Donald Eugene Strandness, a surgeon, realized the potential of Doppler ultrasound in the new field of vascular surgery. He introduced the Doppler methodology to surgeons interested in vascular diseases. The availability of continuous-wave instruments (two classes of Doppler ultrasound instruments are briefly explained

in section 2.2.1) led to immediate attention of clinical applications. Strandness and his associates described the Doppler ultrasound measurement of blood flow in peripheral vessels in an article in 1966. In this article they demonstrate the difference of the waveforms obtained from normal patients and from patients with atherosclerosis.

2.2.1 General View of Doppler Ultrasound

Ultrasound is a sound wave that has frequencies above the audible range of frequencies of human being ($20kHz$). Diagnostic ultrasound instruments emit ultrasound waves to an object of study. Doppler ultrasound systems may be categorized in two groups: Continuous-wave and Pulsed-wave. This classification is based on how the transmitted signal is emitted, being either continuously or in bursts. Continuous-wave instruments use two transducers, one for transmitting the ultrasound and one for receiving the reflected ultrasound. The region of overlap of the beams is the area within which these instruments are sensitive to movement. These instruments have weak range resolution that causes confusion of direction of signals from close vessels. Quantifying the blood flow using these systems is difficult and they have exaggerated sensitivity to vessel walls movement [2].

The primary limitation of Doppler velocity detectors was the incapability to pinpoint the exact location of the moving reflectors that generated the Doppler signal. These instruments could not determine the depth of a blood vessel, nor distinguish varying flow velocities in large vessels and relate them to their location within the vessel lumen [1]. The need for instruments that could effectively measure velocities at specific ranges and obtain profiles across the lumen of a blood vessel led to the development of Pulsed-wave Doppler instruments.

The pulsed Doppler ultrasound is one of the important tools in the study of vessel diseases and the investigation of flow conditions. Due to its non-invasive nature, it has been increasingly used in medicine in the last few decades.

2.2.2 Typical Blood Flow Signals

Doppler ultrasound blood flow studies are based on the analysis of ultrasound signals that are backscattered by moving particles within a vessel. These blood scattering units are mainly the red blood cells (erythrocytes) and cell aggregates. The pulsed ultrasonic Doppler blood flow detector determines blood velocity by measuring the Doppler shift in the frequency of ultrasound.

Doppler shift (or in another words, difference) frequency is defined as the difference between the received and the transmitted frequency. The received frequency is the sum of the reference frequency with a frequency component proportional to the velocity of reflectors, in this case the blood particles. If the angle between the receiving and the transmitting direction of ultrasound is 180°, the relation between the received and transmitted frequency can be formulated as below [2]

$$f_d = f_t - f_r = \left(2.\frac{f_t}{c}\right).v.\cos\theta \tag{2.1}$$

Where f_d represents the Doppler shit frequency, f_t and f_r represent transmitted and received frequency, respectively. c is the velocity of sound in tissue, v is the velocity of the reflectors, and θ is the angle between the ultrasound beam and the direction of motion of the object under study.

In arteries, blood-flow detection by Doppler ultrasound allows the measurement of systolic blood pressure. In veins, blood-flow detection used to be more difficult due to the fact that slower velocities produced lower frequency shift. However this issue was overcome by applying augmentation maneuvers on venous flow. Augmented venous-flow signals make it possible to detect obstructed blood flow caused by venous thrombosis. It can also be used for detection of venous valve incompetence. Doppler ultrasound was found to be able to detect air emboli in late 1960's. It was also proven to be useful in monitoring during open-heart surgery and some neurosurgical procedures [1].

One of the common vascular diseases is stenosis. A stenosis is resulted from an intrusive lesion of blood vessels and could cause the shortage of blood sup-

ply to distal vessels. A vascular stenosis usually causes vortices and turbulence downstream the blood flow. These irregularities in the blood flow can be evaluated to detect and quantify the lesion and its degree [3]. It has been shown that vessel stenosis has a close relation to the abnormal hyperplasia of cells in adjacent vessels, formation of emboli and artery expansion; Therefore detection and estimation of stenotic degree on vessels has a significant importance [4].

2.2.3 Doppler ultrasound and Carotid Artery Surgery

As it was mentioned earlier, atherosclerosis causes stenotic lesions in arteries. A short term treatment of this situation includes minimally invasive angioplasty procedure. This could include application of a stent that physically expands the narrowed arteries. The major invasive surgery is bypass surgery but it provides additional blood supply that goes around the extremely narrowed vessel. One of the main impeller forces in development of Doppler methodology was the rapid increase of reconstructive peripheral vascular surgery during the 1950's and 1960's. Grafting operations to replace or bypass stenotic artery segments as well as endarterectomy to remove luminary structures were receiving huge attention in treatment of atherosclerosis.

During the 1970's, due to reports of high stroke and mortality rates, at community hospitals in the United States, the appropriateness of carotid endarterectomy was questioned. The number of carotid endarterectomy operations performed in the United states significantly decreased from 107,000 in 1985 to 83,000 in 1986. In a period of 5 years from 1986, because of increasing concern of cardiovascular surgery, different international organizations were motivated to indicate the stenotic degree on vessels and appropriateness of surgery. In 1991, European Carotid Surgery Trialists' Collaborative Group known as ECSTCG and North American Symptomatic Carotid Endarterectomy Trial Collaborators (NASCETC) issued their conclusion that symptomatic patients with 70 to 99% stenosis derived significant benefit from operation [1].

By 1992, the decreasing rate of performed carotid endarterectomy that started after 1984, showed an upward trend. After reconfirmation of the utility of carotid endarterectomy, Doppler ultrasound velocity criteria are being established to meet the categories of stenosis relevant to ECSTCG and NASCETC [1].

2.2.4 Doppler Blood Flow Signal Simulator

Physical properties of a Doppler instrument plays a key role on its performance in measurement of blood flow. The other key player that has no less importance is the Doppler signal analysis technique that is employed. It is quite practical to have a source of signals with known characteristics in order to compare the performance of various methods of signal analysis. In this way, one could estimate specific properties of a simulated signal using a suggested signal analysis method and compare the result with the expected values. Moreover the researcher can compare the results of different methods against each other when applied to the same signal. In a situation where an averaged value has to be evaluated, a number of signals could be simulated and stored and using a method or technique obtain the results.

The nonstationary blood flow Doppler signal can be modeled as [5]

$$x_D(t) = A(t)e^{j\Phi_r(t)}e^{j\Phi_d(t)} \tag{2.2}$$

this expression is composed of a random base-band function such as $A(t)e^{j\Phi_r(t)}$ and a frequency shifting function, $e^{j\Phi_d(t)}$. The frequency shifting function has a frequency equal to the blood flow spectral center frequency $f_m(t)$. The random base-band component of the simulated signal can be formulated as

$$A(t)e^{j\Phi_r(t)} = F^{-1}|G(f).N(f)| \tag{2.3}$$

and the phase shifting function that is dependent on the deterministic center fre-

quency curve, $f_m(t)$, as

$$\Phi(t) = 2\pi \int_0^t f_m(t)dt + C \tag{2.4}$$

where F^{-1} denotes the inverse Fourier transform operator. $G(f)$ presents a real zero mean filter function with Gaussian spectral shape and $N(f)$ corresponds to a complex random variable that convey a normal power spectral density and a root mean square (RMS) value of unity. Typically the filter function has a RMS bandwidth of $100Hz$, when simulation of carotid artery blood flow signal is performed.

In the current study the filter function $G(f)$ has a Gaussian shape is given by

$$G(f) = \left(e^{-0.5\left(\frac{f}{b}\right)^2} \right)^{\frac{1}{2}} \tag{2.5}$$

In this Doppler signal simulator, the waveform of deterministic center frequency curve that is fed to the simulator determines the properties of the output signal.

2.3 Spectral Estimators

2.3.1 Fourier Based Methods

2.3.1.1 The Necessity of Time-Frequency Analysis

In the study of a physical phenomena with more than one variable, the dependency and relation of variables with each other within the overall aspects of the phenomena are often important. One example of such a phenomena is any form of time varying spectra. To name such an event, we could mention the quick and dramatic change of frequency composition of light during a sun set. It is practical to devise a distribution that presents the energy or intensity of a signal simultaneously in time and frequency. Consider spectral analysis of audio signal of one hour music concert. Due to the fact that different frequencies are produced by different instruments, naming violin and drum, the overall spectrum of the signal

shows that there are certain music instruments being played. However what can not be extracted from the spectrum is that which instrument is played when. A way to overcome this issue is to represent the signal in a joint distribution of time and frequency.

For better appreciation of the importance of time-frequency analysis, consider 2 signals composed of finite length sine waves. Assume 3 different sine waves at frequencies 16, 19 and 23 Hz. Signal A and signal B are 2 different combinations of these sine waves. Signal A is constructed as an aggregation of the sine wave at 23 Hz first, then 16 Hz and then 19 Hz. On the other side, signal B is constructed as being primarily the sine wave at 23 Hz,then 19 Hz and finally 16 Hz. Signal A and signal B present identical spectrum however by looking at their time domain representation it is observed that they are not identical signals in the time domain. Figure 2.1 presents a comparison of these 2 signals. In this figure, (a) and (b) depict time domain, frequency domain and joint representation in time and frequency domains of signals A and B, respectively.

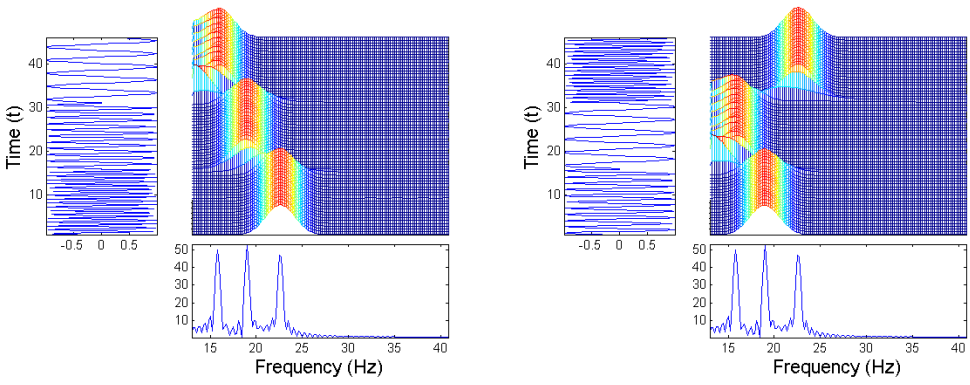

(a) (b)

Figure 2.1: Comparison of signals with different time domain representation and identical spectrum. The top-left plot of (a) and (b) are the time domain representations, the ones in bottom-right are the spectrum and top-right 3-dimensional figures are the colored joint representation of time and frequency of signals.

In some of the real-life applications of digital signal processing a signal, such

as speech signal, is transformed from one domain to another domain. This transformation or mapping is done by means of particular mathematical formulations and has to be information-preserving. Fourier transform is perhaps the most common method to map a signal from time to frequency domain. However the continuous-time Fourier transform (CFT) of a signal fails to provide information about the time order of occurrence of particular frequencies (as it is seen in bottom-right subplots of (a) and (b) as spectrum in figure 2.1).

$$x(t) = \int X(f) e^{j2\pi ft} df \tag{2.6}$$

$$X(f) = \int x(t) e^{-j2\pi ft} dt \tag{2.7}$$

$X(f)$ is referred to as a spectral representation (spectrum) of $x(t)$ with the variable f defined as frequency. Since $X(f)$ and $x(t)$ are uniquely related, it is possible to assume the spectrum as the signal in the frequency domain or frequency representation [6]. To overcome the aforementioned issue of order of occurrence in time, a spectral representation that includes some explicit dependence on the time is needed (top-right subplots of (a) and (b) as in figure 2.1). A mathematical function that formulates a mapping process from time to frequency domain of the form $X(f,\tau)$ in which f corresponds to frequency and τ to time could be the solution. In this process, the signal is being analyzed at certain frequencies, to be called frequency bins. The result of such a transformation is conveying values for different frequency bins at each and every time instant. In another words, wherever there is presence of a particular frequency, the result is representing its estimated value.

2.3.1.2 The Short-Time Fourier Transform and Spectrogram

In analyzing the frequency content of a signal, in order to obtain a finer localization in time, one could choose smaller segments in time. However it must be taken into account that reducing the length of time segments is subjected to limitation. The reason behind this limitation is that after certain amount of narrowing the time slice, the spectrum presents no relation to the spectrum of the original

signal. This issue can be explained as parsing a signal into short duration signals, causes the constructed segments to have inherently large bandwidth. The spectra of such short duration signals convey altered information concerning the properties of the original signal [6]. This limitation is called uncertainty principle and it is applied to the small segments in time to be analyzed, rather than to the whole duration of the signal.

In order to analyze a given signal at time t, one could emphasize the signal at that time and suppress the signal at other instants of time. This could be done by multiplying the signal by a window function, $h(t)$, centered at the moment t, that results in a modified signal:

$$x_\tau(t) = x(t)h(t-\tau) \tag{2.8}$$

The resultant modified signal is function of two times. First it is a function of moment in the time the analysis is being done, τ, second the running time, t. The window function is the mathematical function that is used to segment the signal over time. There are numerous window function being used in signal processing applications and each one has specific properties. Throughout the employment of a window function on a signal, power properties of the window function are affecting the result. Whenever an interpretation and estimation has to be done on the Fourier transform of a windowed signal, special care must be taken into account on the effect of the window function. The selection of the window function is based on the fact that it is needed to leave the signal unaltered to some extent at the time τ of interest and suppress the signals for all the values distant from that moment.

$$x_\tau(t) \sim \begin{cases} x(t) & \text{for } t \text{ near } \tau \\ 0 & \text{for } t \text{ far away from } \tau \end{cases} \tag{2.9}$$

The term ”window” originates from the fact that a portion (small segment in time) of the signal is being observed. In an analogy a small portion of a scenery is seen from a window and the rest is not considered in the observation.

Since the modified signal emphasizes the signal around time τ, the Continuous Fourier Transform (CFT) or spectrum will reflect the distribution of frequency around it; this could be shown as equation 2.10

$$X_\tau(f) = \int e^{-j2\pi ft} x_\tau(t) dt \tag{2.10}$$

Substituting $x_\tau(t)$ from equation 2.8 in equation 2.10 results in

$$X_\tau(f) = \int e^{-j2\pi ft} x(t) h(t-\tau) dt \tag{2.11}$$

Therefore the energy density spectrum at time τ can be written as below [6]:

$$P_{SP}(\tau, f) = |X_\tau(f)|^2 = \left| \int e^{-j2\pi ft} x(t) h(t-\tau) dt \right|^2 \tag{2.12}$$

It is possible to obtain energy density spectrum for each different time. The totality of these spectra is the time-frequency distribution , P_{SP}. This time-frequency distribution is often called "spectrogram". Since it is desired to analyze the signal around time τ, a window function that has a peak around time τ has been chosen. Hence the name short-time as the modified signal is short in duration and its Fourier transform, Equation 2.11 is called the short-time Fourier transform. It is a convention to represent CFT of signal $x(t)$ at moment τ by $X_\tau(t)$ or in another form by $X(\tau, f)$.

Short-time Fourier transform or simply STFT is based on the simple idea of parsing a signal into small time segments and then Fourier analyze each segment to ascertain existence of frequencies in each segment. The totality of such spectra indicates how the spectrum is varying in time. One of the most widely used method to study non-stationary signals is short-time Fourier transform [6]. Mo and Cobbold [7] state that Doppler signal can be considered as wide-sense quasi-stationary during a short time interval therefore application of STFT on it would be feasible. It is worth to mention that the result of STFT is strictly tightened to the properties of the used window function.

In some situations, it is convenient to express the STFT in another form, for

instance as an integral in the frequency domain, that is:

$$X(\tau, f) = e^{-j2\pi f\tau} \int e^{j2\pi ft} X(u)H(u-f)du \tag{2.13}$$

where $X(u)$ and $H(u)$ are Fourier transforms of $x(t)$ and $h(t)$, respectively, and u is a dummy frequency variable. We can interpret this function as the frequency-shift of the inverse continuous Fourier transform of $X(u)H(u-f)$. If $H(u)$ is chosen in a way to present a low-pass filter in frequency, therefore $X(u)H(u-f)$ is the CFT of $x(\tau)$ being filtered by a bandpass filter with the shape of $H(u)$. Since the bandpass filter is translated in frequency, it is centered at f instead of 0. The factor $e^{-j2\pi f\tau}$ in equation 2.13 is to shift the filtered output back to zero. In this way, STFT can be seen as a process of filtering a signal with a bank of filters, and then frequency shift each output back to zero. These filters have constant bandwidth but centered in different frequencies.
The STFT can be written as a convolution in time:

$$X(\tau, f) = e^{-j2\pi f\tau} \left[e^{j2\pi f\tau} x(\tau) * h^*(-\tau) \right] \tag{2.14}$$

Where symbol $*$ denotes the convolution integral. Convolution integral is defined as:

$$u(\sigma) = \int \upsilon(\lambda) w(\sigma - \lambda) d\lambda \equiv \upsilon(\sigma) * w(\sigma) \tag{2.15}$$

As it was mentioned earlier, it is not possible to narrow the time slice unconditionally. Consider choosing $h(t)$ as short as possible in time. Doing so, in the limit $h(t) = \delta(t)$, where $\delta(t)$ is the Dirac delta function. This function transforms to frequency as $H(f) = 1$. Substituting it in equation 2.11, shows that $X(\tau, f) = e^{-j2\pi f\tau} x(\tau)$ that is simply the original signal $s(t)$ translated down in frequency. This transformation absolutely preserves the time information, while on the frequency it provides no information whatsoever. It is possible to show that [8] as a consequence, the uncertainty principle restricts values of Δt and Δf as time and frequency resolutions of STFT to satisfy $\Delta f \Delta t = C$. In which C is a nonzero value whose precise value depends on the definition of width that is selected. Therefore it can be concluded that once the function $h(t)$ is chosen, the time and frequency resolution of STFT are fixed for all the values of t and f [9].

2.3.2 Continuous Wavelets Transform

An inevitable characteristic of STFT is that both time and frequency resolution are fixed over the entire time-frequency plane. The time resolution is fixed as a consequence of $h(t)e^{-j2\pi ft}$ regardless of any value of f. Consequently, $\Delta f = C/\Delta t$ is also fixed over the entire plane. There are certain situations in which it is desired to overcome fixed resolutions. Consider analysis of a signal with 2 sets of components: short-lived high frequency features that are closely spaced in time whereas the other ones are long-duration low frequency components that are closely spaced in frequency and complete their cycles in a large time interval. A proper transform of such a signal must have enough sufficient time resolution to distinguish the high-frequency features, while it has to be with enough frequency resolution to separate closely-spaced low frequency ones. Satisfying these two requirements simultaneously, is not in the scope of the STFT.

One suggestion could be the application of two STFT with different $h(t)$: to meet the time resolution requirement, use a short-lived $h(t)$ with a small value of Δt, then a long-duration $g(t)$ for good frequency resolution. The other option could be such a time-frequency representation that has variable time-frequency resolution; good time resolution for high frequencies and good frequency resolution for low frequencies. To address the issue of the compromise between time and frequency resolution, Continuous Wavelet Transform would be suitable. As the resolution is not fixed in this form of transformation, it is categorized as "multi-resolution" transformation. The multi-resolution transformation is done by decomposition of a given signal on a set of shifted (by amount of τ) and scaled (by s) function derived from a predefined prototype, $\Psi(t)$. This prototype function is called mother wavelet function. The wavelet has to be chosen in a way that by means of appropriate shifting and scaling, proper estimation on the signal could be done. The CWT is expressed as

$$CWT(\tau, r) = \frac{1}{\sqrt{|r|}} \int x(t)\Psi^* \left(\frac{t-\tau}{r} \right) dt \tag{2.16}$$

Where t and τ represent the time, $x(t)$ is the time domain signal being analyzed, r denotes the scale parameter and $\Psi^*(t)$ is the complex conjugate of the wavelet function. The factor $1/\sqrt{|r|}$ is used to ensure energy preservation. Scale parameter is a concept used in wavelet theory and it is the counterpart of frequency. Scale parameter and frequency f are related by $r = f_0/f$, where f_0 represents the central frequency of the wavelet's Fourier transform. Likewise STFT, it is possible to express CWT as an integral in the frequency domain, that is [9]:

$$CWT(\tau,r) = \sqrt{|r|}\int S(u)\Psi^*(ur)e^{j2\pi f\tau}du \tag{2.17}$$

Where $S(u)$ and $\Psi(u)$ correspond to the CFT of $x(t)$ and $\psi(t)$ respectively. Also as convolution in time domain

$$CWT(\tau,r) = \frac{1}{\sqrt{|r|}}\left[x(\tau) * h^*\left(\frac{-\tau}{r}\right)\right] \tag{2.18}$$

To better grasp how the CWT differs from the STFT, compare the terms corresponding to filter function in equation 2.14 and equation 2.18 that are STFT and CWT in the form of convolution in time. In the case of CWT we can confirm that the width of $h(\tau/r)$ is not fixed, but rather dependent on the value of r. Reminding the scaling operation in one domain on a given signal, one can say that $h(t/2)$ has twice the width of $h(t)$ while $h(2t)$ has half the width of $h(t)$. Since time resolution of the CWT is dependent on the width of function $h(\tau/r)$, as r decreases, the function gets narrower in time and in return the time resolution improves. In contrary as r increases, the time resolution is degraded, but the frequency resolution is improved as the quantity $\Delta t\Delta f$ has to remain constant.

In the same manner that filter bank for STFT was defined previously, we can invoke the same concept for CWT. In this case CWT could be interpreted as a process of filtering a given signal with a bank of filters with fixed relative bandwidth or varying absolute bandwidth as one version of CWT. Matos et al. [10] investigated the properties of results of CWT using fixed and varying absolute bandwidth. In our study both versions have been implemented and results were compared along with the results of STFT. The relative bandwidth (BW_{rel}) of a fil-

ter (or a function) is defined as the ratio between the absolute bandwidth (Δf) of the bandpass region surrounding the filter's center frequency and the center frequency (f_h) itself. Based on this definition a Q factor is defined as the inverse of the relative bandwidth:

$$BW_{rel} = \frac{\Delta f}{f_h} = \frac{1}{Q} \tag{2.19}$$

The result obtained from CWT is in the scale-frequency format. However to comply this result with the ones obtained from STFT, a time-scale to time-frequency mapping has to be employed. Since during the CWT process, $\psi(t)$ was sampled to $\psi[n]$ using sampling rate of Fs_x, a ratio between the sampling rate of $x[n]$ (Fs_x), and Fs_h is defined. Equation 2.20 presents the relation between scales and frequencies.

$$s = \frac{k}{f} \tag{2.20}$$

where k is

$$k = \frac{F_{s_x}}{F_{s_h}} \tag{2.21}$$

Strictly speaking, the CWT is a time-scale representation and it has to be mentioned that this mapping (proposed by Teich et al. [9]) is the way to interpret the result of CWT in compliance with STFT.

2.3.3 Computing the PSD

2.3.3.1 Power waveform

Application of STFT on a given discrete signal, that is application of FT to the time slices of the signal, will result in spectral density of the signal; regarding each instant of time, it could be formulated as

$$S(k) = \sum_{n=0}^{N-1} x_w(e)^{-j2\pi kn\Delta T} \tag{2.22}$$

where n is an instant of discrete time and k is frequency, x_w is the application of a window function on the signal, ΔT is the duration of time being processed and N

is the number of frequency points used. Leiria [11] states that using equation 2.23 we can calculate the corresponding power density spectrum

$$P(k) = \frac{1}{N} |S(k)|^2 \tag{2.23}$$

In order to make sure that the power spectrum is an average value over the time slice being observed as opposed to a function of the window size, the factor $\frac{1}{N}$ is being used in the expression. In the case where the window function applied to the signal is a rectangular window, equation 2.23 is a good approximation of the PSD [11], however in the case of other window functions (for instance hamming) that do not demonstrate a unitary power density spectrum, the power density of the applied window has to be introduced in the expression as

$$E_N = \frac{1}{N} \sum_{n=0}^{N-1} w^2(n) \tag{2.24}$$

which means that equation 2.23 would be rewritten in the form of

$$P(k) = \frac{1}{NE_N} |S(k)|^2 \tag{2.25}$$

and subsequently the power density expression regarding each instant of time and frequency could be written as below

$$P(n,k) = \frac{1}{NE_N} |S(n,k)|^2 \tag{2.26}$$

and the variation of the power over time is

$$P(k) = \sum_{k=0}^{N-1} P(n,k) \tag{2.27}$$

2.3.3.2 Mean Frequency waveform and Bandwidth

The mean frequency for each instant of time is calculated using the power density at each instant and weighted regarding the frequency bins being used and

averaged [5].

$$\tilde{f}_m(n) = \frac{\sum_{k=0}^{N-1} f(n,k) \cdot P(n,k)}{\sum_{k=0}^{N-1} P(n,k)} \tag{2.28}$$

where n and k correspond to discrete time and frequency, respectively. $f(n,k)$ denotes the frequency value corresponding to moment n and frequency bin k. Similarly the spectral RMS half bandwidth estimation is computed using the equation below.

$$\tilde{b}(n) = \sqrt{\frac{\sum_{k=0}^{N-1} \left(\tilde{f}_m(n) - f_k\right)^2 P(n,k)}{\sum_{k=0}^{N-1} P(n,k)}} \tag{2.29}$$

Chapter 3

Spectral Methods Applied

3.1 Simulation of Blood Flow Signals

Using the expression of $\Psi(t)$ (see 2.4), one can obtain a Doppler simulated signal based on a desired form of spectral center frequency variations. In fact any arbitrary form of curve could be used with this function. However decision was made to choose a curve from literature that has been developed and investigated previously by scholars. This center frequency is depicted in figure 3.1 and is derived from a convective velocity waveform. This velocity waveform obtained by assessment of Doppler ultrasound blood flow on common carotid artery during a cardiac cycle. The velocity waveform incorporates spectral width and power increase that is resultant from flow disturbance. Moreover the waveform conveys time-localized rapid variations in frequency compelled by the passage of vortices [3]. This center frequency curve was proposed by Wang and Fish [12].

3.2 Spectral Estimation Methods

Spectral estimation methods that were investigated in this study were Short-Time Fourier Transform (STFT), and Continuous Wavelet Transform (CWT). The STFT implementations were mostly based on the functions available from MATLAB. A noise reduction technique was proposed. The STFT method to eliminate the accompanying noise of the simulated signal as well as the clinical signals was

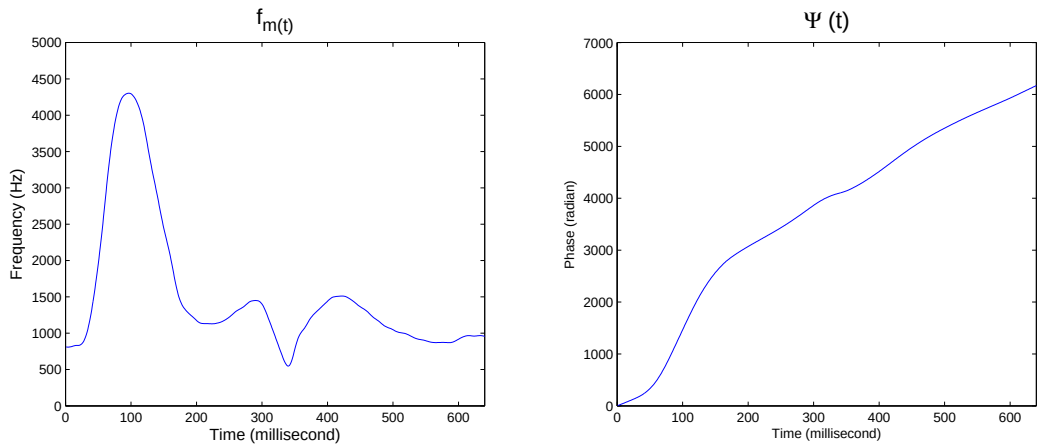

Figure 3.1: Deterministic center frequency curve $f_m(t)$ (left) similar to that obtained from the common carotid artery, and corresponding $\Psi(t)$ curve (right)

enhanced. The CWT routines and codes were adopted from a previous work done by Matos et al. [10]. In this study, two forms of CWT were investigated: varying bandwidth filter and fixed bandwidth filter. These methods were applied to simulated signals with different levels of noise.

Rangaraj [13] states that synchronized signal averaging can separate a repetitive signal from noise without distorting the signal. If the noise is random with zero mean, averaging will improve to SNR. He mentions methods to apply the synchronized averaging on different clinical signals. For instance in the case of ECG, detecting the QRS complexes and using their position to align the waveforms to synchronized averaging would be an option. In the case of simulated signals, it is simply done by performing the desired number simulations. The added random noise in the simulator used in this study has zero mean. Thus averaging on a number of simulated signals can be applied to reduce the noise. It was decided to obtain the results from 100 simulated signals. In order to quantitatively compare the methods, center frequency and bandwidth of signals were evaluated and compared against the deterministic ones.

3.2.1 STFT Based Method

In the processing of clinical signals that are acquired in a real-life situation mostly there are non-zero values at instants of time-frequency. Logically part of these values are generated by the original source of the signal; for instance in studying blood flow using Doppler ultrasound the blood particles that backscatter the Doppler ultrasound to be detected by the ultrasonic detector. The rest of the values of occurred frequencies that are relatively small, correspond to the noise and any undesired acquired information. The idea at this point of study was to establish a series of routines to obtain time-frequency representation of a given signal. Then manipulation was required in a way so that acceptable results, i.e. center frequency and bandwidth parameters, could be extracted from the signal.

Since MATLAB provided 'spectrogram' function, it was decided to use this function. The function's input variables were modified in order to obtain a time-frequency representation of signals. Then on this intermediate results, the developed cancellation methods could be applied. Following this procedure, spectral parameters, i.e. center frequency and bandwidth could be extracted. The syntax of the command used is as below

```
spectrogram(signal,window,noverlap,F,fs,'yaxis')
```

where `signal` is a one dimensional real input signal, `window` is the size of the used window in data points. `F` is the vector of frequencies and `fs` is the sampling frequency of the input signal. This function plots a 2-dimensional graph where a colored pixel represents the spectral power occurring for a particular pair of instant of time and corresponding frequency. The redder spots represent higher power values while the bluer ones represent lower values of the power spectrum. To obtain a plot where the horizontal axis corresponds to time and the vertical axis to frequencies, as it is used in typical Doppler blood flow signal representations, the `'yaxis'` had to be added at the end of the list of inputs; otherwise, the axes will be swapped.

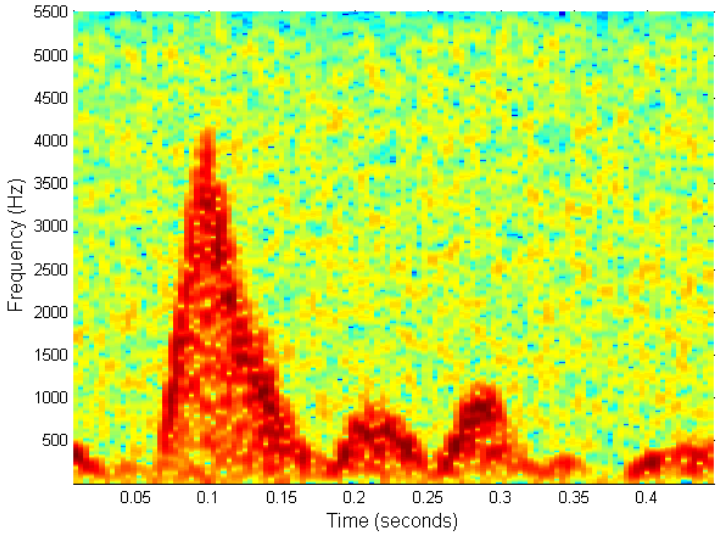

Figure 3.2: Spectrogram of 5000 data points (roughly one cardiac cycle) of a clinical Doppler signal.

Another possible format of '`spectrogram`' command is

```
[S,F,T,P]=spectrogram(signal,window,noverlap,F,fs,'yaxis')
```

This command produces a positive and negative complex valued matrix '`S`', vectors '`T`' and '`P`' and a positive real valued matrix '`P`', as the power spectral density. For the case of real input signal, one-sided modified periodogram estimate of the PSD of each data segment will be obtained. The matrix '`S`' is the short term Fourier transform of the input signal. Vectors '`F`' and '`T`' are frequency and time vectors respectively. Length of '`F`' is the same as the number of the frequency points of the output. Matrices '`S`' and '`P`' have the same size. The 'columns' and 'rows' of these matrices are of the length calculated as in equation 3.1.

$$\begin{aligned} rows &= size(F) \\ columns &= fix\left(\frac{nsignal - noverlap}{window - noverlap}\right) \end{aligned} \tag{3.1}$$

in which '`size`' and '`fix`' are MATLAB functions. '`nsignal`' is the length of the input signal and '`window`' and '`noverlap`' are the lengths of each segment and overlapping of two adjacent segments, respectively.

3.2.2 Clinical Data Noise Reduction Technique

After applying the '`spectrogram`' function of MATLAB, a time-frequency representation of a given clinical signal can be obtained, from which relevant information, may be obtained. The obstacle is that this time-frequency representation contains both the information from the Doppler blood flow signal and the accompanying noise with it. To eliminate the noise from the spectrogram of a given clinical signal and to estimate spectral parameters such as center frequency and bandwidth, a noise cancellation technique has been developed.

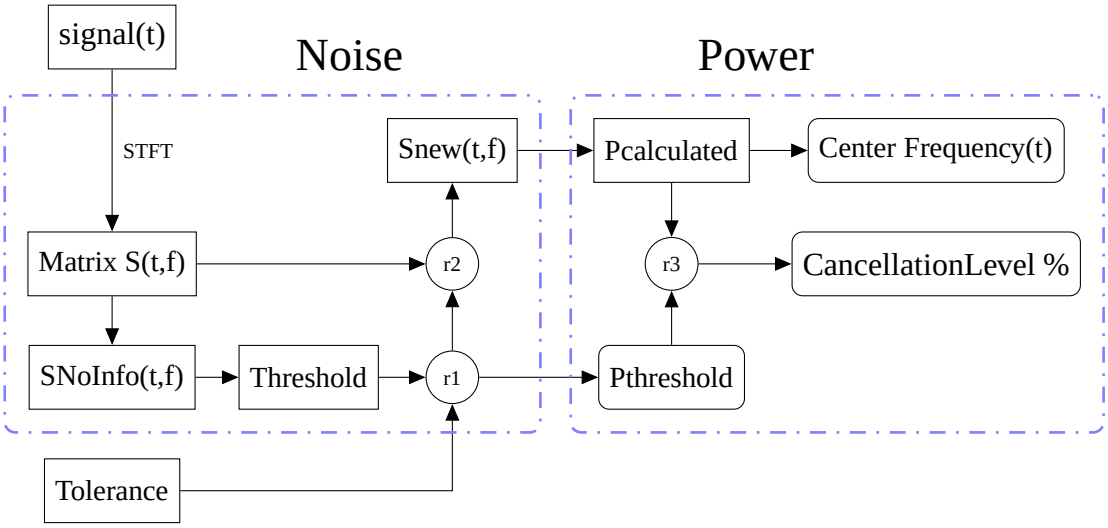

Figure 3.3: Block diagram of implemented MATLAB routines to eliminate noise from STFT of a given input. The input signal is an audio file of Doppler signal. The operator of a system based on this block diagram adjusts the value of *Tolerance*. The operator also involves in selection of the region in the STFT corresponding to the $SNoInfo$. *Pthreshold* presents the threshold of noise elimination (as a power value), $center\,frequency$ is the estimated center frequency of the spectrogram and $CancellationLevel$ quantifies the amount of noise cancellation procedure. Outputs are depicted with rounded-corner rectangles.

Figure 3.3 presents the block diagram of the implemented MATLAB routines concerning this study. The sets of operations on the input file and the intermediate outputs are divided in two groups. In the first half, the noise is identified and isolated and then removed from the signal. This part is indicated with the

left hand side dashed rectangle in figure 3.3 and is named “Noise”. The operation within this part are being explained in section 3.2.2.1. The second half of the operations are dealing with the power waveform and power calculations. The final outputs are obtained in this part. The right hand side dashed rectangle in figure 3.3 presents the block diagram of the operations related to this part. Section 3.2.2.2 corresponds to the second half of the operations.

Outputs in this diagram are indicated with rounded-corner rectangles. A time domain signal is forming the input of this series of routines. In the first place the STFT is applied on the input. Within the resultant time-frequency representation, particular region of frequencies is marked as the noise portion. This portion that does not correspond to the blood flow signal is called ’SNoInfo’. Selection of this portion requires the decision of user of the system. The user can select this region by observing the graphical representation of the STFT. Based on SNoInfo, a threshold is defined. The threshold along with a tolerance to ensure a secure error margin is used to eliminate particular values in the time-frequency representation of the input. In this figure, circle ’r1’ represents a simple multiplication function and circle ’r2’ is an implemented MATLAB routine that eliminates any value in a given matrix (real complex valued) that is less than a defined value (product of Threshold and Tolerance). The result of the elimination is called ’Snew’. The power matrix is obtained using the matrix Snew. This power matrix is called ’Pcalculated’ and only represents the power of the values corresponding to the blood flow signal and not the noise. Using the obtained matrix power, center frequency of the Doppler signal could be estimated. As an output, threshold is presented in the form of power and is called ’Pthreshold’. This value indicates the power threshold so that power values above it are considered as the values corresponding to the blood flow. In order to present the level of noise reduction applied on the input signal, a value as ’CancellationLevel’ in percentage is defined.

In the following subsections, the noise reduction technique terms and procedure will be described. From now onwards, the ’`spectrogram`’ clinical Doppler signal’s input, containing the blood flow signal plus noise will be called ’clinical signal’; when only the blood flow is considered, the term ’pure signal’ or simply

'signal' will be used. The term 'signal' might be used in contexts related to both time and frequency domain.

3.2.2.1 Noise Identification, Separation and Reduction

In this subsection, the terms corresponding to the time-frequency representation of a signal, the portion related to noise and the procedure to eliminate it, are being explained. The matrix corresponding to the time-representation of a clinical signal is being represented as a 2-dimensional matrix and then the area belonging to the noise is being identified and separated. A graphical comparison on different levels of noise for a simulated signal based on the colored spectrogram is presented. Then particular values are defined to be used to eliminate certain level of noise.

Matrix S is a positive and negative complex valued matrix in which the rows correspond to the frequencies and the columns to instances of time. In the case of figure 3.2 the '`spectrogram`' function was set for 1024 frequency points, 190 data points for the window length and overlap of 120 data points to calculate spectrogram of 5000 data points of a portion of a clinical signal. Using '`surf`' function of MATLAB, a 3-dimensional plot of the real part of the matrix '`S`' would resemble figure 3.4.

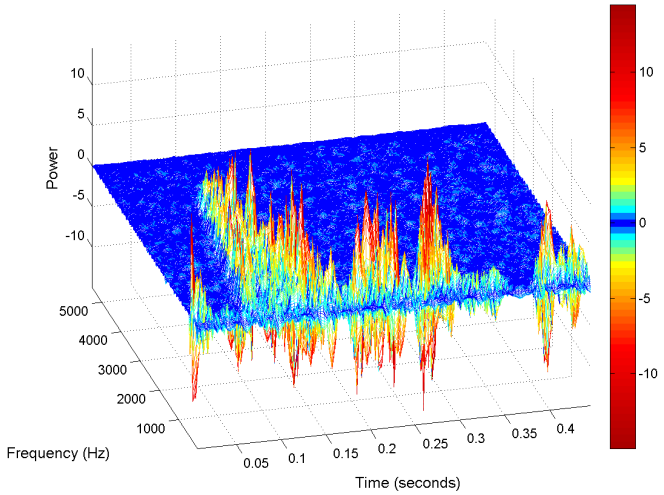

Figure 3.4: 3-dimensional representation of the real part of matrix 's'.

BackGroundArea in the plot representing matrix 's' (figure 3.4), there is an area that depicts the signal, or in another words, existence of specific frequencies at each time instant related to the pure signal. However in the rest of the plot one can see a spinous area corresponding to the noise. This region has less reddish but rather darker color. From now on this area and its corresponding part of the matrix 's' will be named BackGroundArea. The level of the spines in the BackGroundArea is relatively smaller for the signals that have a less noisy time domain representation (i.e. having more definitive sound by listening to their audio file) in comparison with clinical signals with more noisy audio.

In figure 3.5 a comparison of color tone of background areas can bee seen. In each subplot of this figure, different values of Gaussian noise were added to a simulated signal. Therefore the signal to noise ratio of these signals are different. Afterwards their spectrogram were obtained. In 3.5a the spectrogram of simulated signal is represented with no noise, so that more bluer BackGroundArea is expected; whereas in 3.5d, due to the amount of the added noise, the same simulated signal has $SNR = 2dB$

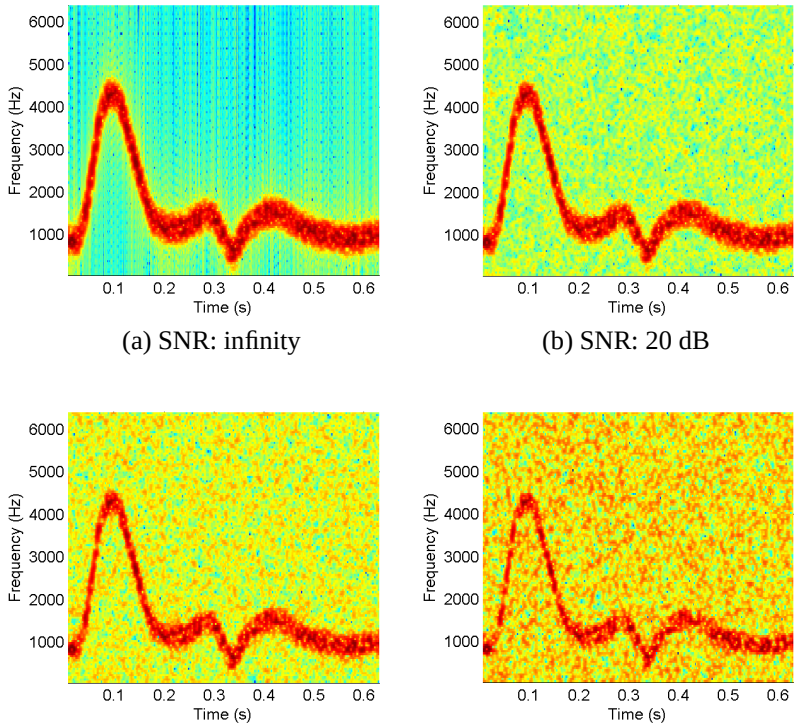

(a) SNR: infinity (b) SNR: 20 dB

(c) SNR: 10 dB (d) SNR: 2 dB

Figure 3.5: Spectrogram of a simulated signal with 4 different levels of noise; three different levels of Gaussian noise were added to original signal without noise in (a), so that resulted in SNR of 20 dB (b), 10 dB (c), and 2 dB (d).

SNoInfo For all the clinical Doppler signals under analysis on this work, it is possible to point to a region of the matrix 's' that covers a range of frequencies in all instants of time in which the frequencies related to the signal do not exist. In these parts we only have the background area. This area is called SNoInfo and can be seen as a matrix. For instance in figure 3.4 this area could be roughly addressed as the area between 4500 to 5000 Hz. This area has approximately the same color tone of the rest of the BackGroundArea. Thus it could be used to give an insight of the statistical characteristic of the background noise or BackGroundArea. It is practical to use magnitudes of elements of SNoInfo matrix to calculate the root mean squared (RMS) or the mean value of the BackGroundArea. This calculated value could be used to distinguish between values of elements of matrix 's' that either belong to the BackGroundArea (the noise) or to the signal itself.

Threshold Having the RMS of the matrix SNoInfo already calculated, one can define a threshold that could be used to assign elements of matrix 's' to BackGroundArea or the pure signal. Based on this threshold the matrix 's' will be processed to eliminate the noise of the clinical signal. Needless to mention that the matrix 's' has positive and negative values. Consequently the elements with their 'absolute' value less than the Threshold will be assigned to the BackGroundArea.

Tolerance In a time-frequency representation, instants of time-frequency corresponding to the pure signal mostly demonstrate a significantly larger magnitude (redder pixel in spectrogram) in comparison to the BackGroundArea. Figure 3.6 represents the spectrogram of a portion of a clinical signal in the left hand side and magnitude of occurred frequencies at an arbitrary instance of time within that portion in the right hand side. In this figure it can be seen that at this particular instant of time, frequency variation above (approximately) 1100 Hz have magnitude values in the range of -0.2 to 0.2. These frequency variations correspond to the time-frequency values located at the BackGroundArea. However looking at frequency variations between 200 Hz and 1100 Hz, roughly it can be said that the magnitudes are between -5 and 5 and there are frequency peaks taking place with magnitudes -12 and 12.

In order to make sure the implemented MATLAB routines will effectively eliminate the values of spikes in the BackGroundArea, the value of Threshold is multiplied by a positive real number designated by Tolerance. This way one can have a secure error margin. Depending on the magnitude of the difference between the values of the frequency of the signal and the values of the spikes of the BackGroundArea, this Tolerance could be adjusted. The value of Tolerance should be small enough to leave the spikes related to the pure signal intact and eliminate (ideally) all the other spikes that belong to the BackGroundArea. In another words, the value of Threshold as well as Tolerance changes from a given clinical signal to another.

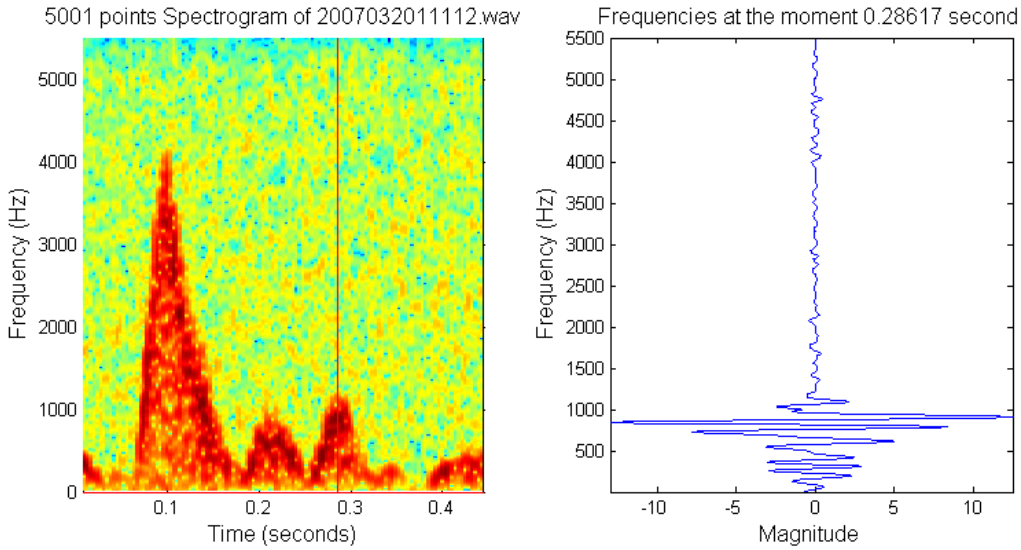

Figure 3.6: Spectrogram of a portion of a clinical signal (left hand side) where a particular time instant (0.286 second) is pinpointed by a red line; right hand side of figure represents the magnitude of frequency variations at that time instant.

Snew Once established the values of Tolerance and Threshold and after obtaining their product, within the matrix 's' values with absolute values less that the previously referred product can be eliminated. Ideally, this action will result in a matrix where all the values in its BackGroundArea are eliminated (turned into zero). This "cleaned" signal is called Snew. Figure 3.7 illustrates the frequency variations observed for a particular time instant (0.286 second as exemplified in figure3.6) before (left plot) and after (right plot) the Snew calculation. In the case of this figure, the Threshold value is set to 0.2003 and the Tolerance to 4 resulting in elimination of values between -0.8014 and $+0.8014$. It can be seen that this range is distinguishably smaller than the average magnitude of the frequency variations belonging to the signal. In this example it is possible to assume that the range of frequencies belonging to the BackGroundArea is approximately the range of frequencies higher than 1100 Hz. In this range the maximum value of the spikes is 0.6020 which is still smaller than the product of the Threshold and Tolerance. In Figure 3.7 we can verify how the frequency values corresponding to the signal are left untouched throughout the process.

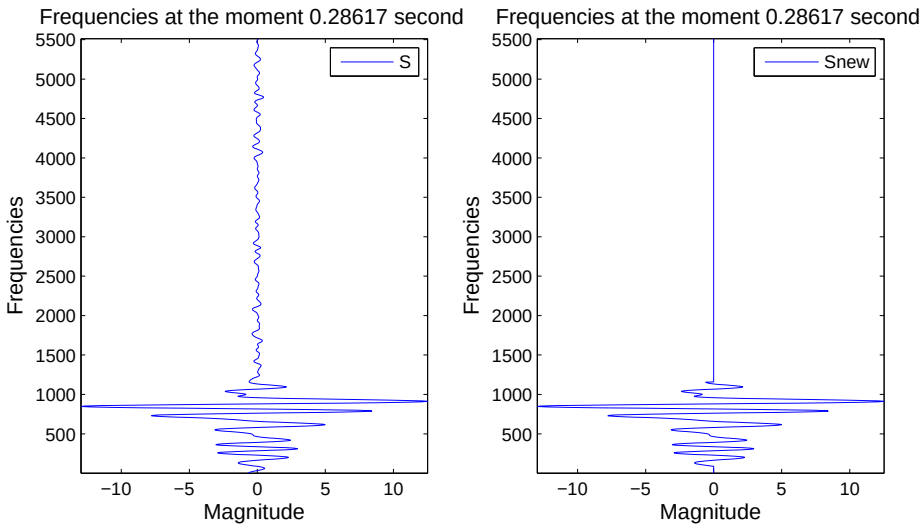

Figure 3.7: A particular time instant of clinical signal of figure 3.6 before (left hand side) and after Snew calculation (right hand side).

3.2.2.2 Power Spectral Calculation

In this subsection, the terms related to power spectral calculations are being explained. Primarily output of the MATLAB function '`spectrogram`' is presented. Then power spectral calculation applied on a noise reduced input is being explained. Finally a threshold value in the sense of power and a term as *CancellationLevel* are introduced. The *CancellationLevel* quantifies the amount of noise reduction applied to a given input; it gives an insight on the level of reduced noise regarding RMS of the pure signal.

Pmatlab Is a matrix with the same size as the matrix '`S`' presented as an output of the later format of the MATLAB function '`spectrogram`' as explained in 3.2.1.

Pcalculated Is a matrix with the same size as the matrix *Pmatlab* that could be obtained applying equation 2.26 on the matrix '`S`'. The window that has been used is the Hamming window. Aydin and Markus [14] compared six different window types (rectangualr (Boxcar), Bartlett, Hanning, Hamming, Blackman and Gaussian) and the results showed that Hamming and Bartlet windows give the highest EBR. EBR is "the ratio of embolic signal intensity to background intensity". It is

worth to mention that the MATLAB routines were implemented in a way that the window type could be easily changed. Since these windows are provided by MATLAB itself, it is possible to choose for this or any other window type throughout the procedures. The number of frequency points used in the case of figure 3.7 is 1024 points. In another scenario, applying equation 2.26 on the matrix *Snew* we can have the matrix of power values from the denoised time-frequency representation.

PThreshold Having a MATLAB code developed to calculate matrix *Pcalculated* from the matrix *S*, we can represent the Threshold value (explained in section 3.2.2.1) in the form of power value . For the case of figure 3.7, assigning the Threshold and Tolerance values mentioned in section 3.2.2.1, the Pthreshold is $9.8254 \times 10^{-}7$. Meaning that instants of time-frequency having power less than this value are eliminated.

Power Waveform Obtaining the matrix *Pcalculated* from the matrix *Snew*, by summing its values at each instant of time (columns) we can obtain a power waveform that represents the power waveform over time (see equation 2.27). This waveform is demonstrating the power which is related to the signal. The power values from the BackGroundArea are omitted from it. It is obvious that doing the same procedure on *Pmatlab*, matrix of values of powers at each instant of time-frequency, results in a waveform that is containing the information of the signal itself and the BackGroundArea too.

CancellationLevel From the matrix *Snew*, one can calculate $Pcalculated$. Then based on this matrix, by using equation 2.28 we can obtain the mean frequency waveform. Comparing this waveform with the mean frequency waveform obtained from the matrix *S* it can be seen that by adjusting $Thresshold$ and $Tolerance$ that results in adjustment of $Pthreshold$, we can obtain an acceptable definition of the mean frequency waveform of the signal. The $CancellationLevel$ is a value represented in percentage corresponding to the ratio between $Pthreshold$ and RMS of the values of the matrix $Pcalculated$. The values existing in the matrix $Pcalculated$ are values that are above $Pthreshold$, thus the $CancellationLevel$ is

a value that is related to both *Pthreshold* and the values belonging to the power of instants of time-frequency not belonging to the BackGroundArea. For the case of figure 3.7 this value is small, as it might be expected, and that is only 3.46%. This tenuity is due to the fact that for this particular signal, the BackGroundArea has relatively small level.

3.3 Wavelet based Method

As it is stated in chapter 2, decision was made to study the implementation of two forms of filter banks to use them in Continuous Wavelet Transformation algorithms: varying bandwidth filter (according to the frequency being analyzed) and fixed bandwidth filter. The MATLAB code implementation of CWT was based on the fast-CWT algorithm proposed by Jones and Baraniuk [15]. Three levels of Gaussian noise were applied to simulated signals in order to simulate signals with different SNR: infinity (no noise), 20 dB and 10 dB. Using these algorithms, CWT of 100 signals were estimated, center frequency curves were obtained and then averaged. Finally this average was compared with the deterministic center frequency waveform used to obtain the simulated signals in the first place. To ease analysis of these curves, the resultant center frequency waveform was divided into 3 region: Mountain, Valley and Steppe. for each region, the bias was studied using 3 parameters: maximum value, minimum value and average. Based on these values and requirement of a specific application, we can decided for fixed or varying bandwidth filters.

3.3.1 Wavelet Base

The wavelet base that was used in this part of the study was High-Q Morlet wavelet that is well concentrated both in time and frequency. This wavelet can be written in the following form [9]

$$\psi(t) = exp(jct).exp(-\alpha t^2/2) \tag{3.2}$$

In this expression parameter c was set to 2π so that the wavelet would be symmetrical around $f = 1Hz$. Parameter α was tested by Matos et al [10] to obtain the best estimation results. Decision was made to maintain the value, that is 0.0123. The real part and the magnitude of the Fourier transform of this function is shown in figure 3.8. There are many oscillations (>50) in the real part and a duration of approximately 60 time units was presented. For the chosen values of c and α the $\psi(t)$ function resembles a windowed sinusoid and $\Psi(f)$ is a narrow bandpass filter centered at $f = 1Hz$. This wavelet has a narrow relative bandwidth (see equation 2.19) and it is readily calculated [9] to be:

$$BW_{rel} = \frac{2\sqrt{2\alpha}}{c} \tag{3.3}$$

that is 0.050 in our study. This value of relative bandwidth results in a $Q = 1/0.050 = 20 \gg 1$ and hence the name High-Q.

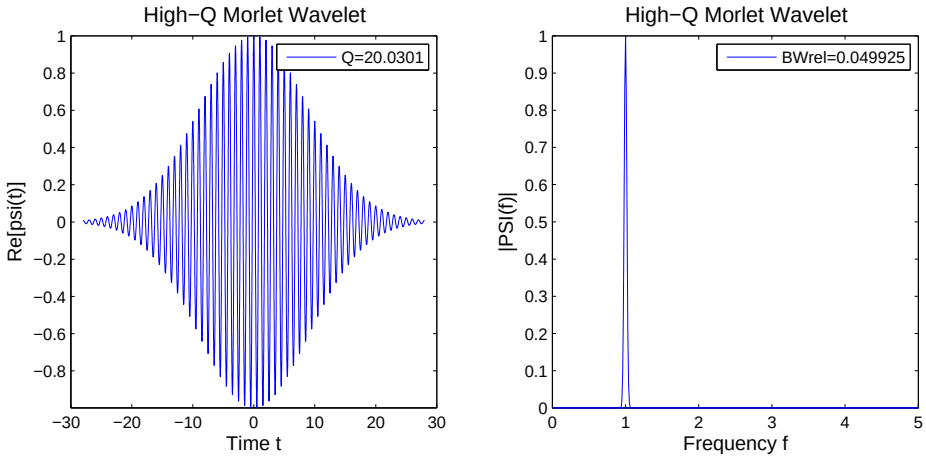

Figure 3.8: High-Q Morlet in time domain (left hand side) with time unite t, and frequency domain (right hand side).

By choosing $\alpha = 0.4$ and maintaining $c = 2\pi$, we can have a low-Q Morlet as in figure 3.9 that is again centered at $f = 1Hz$. In this case the Q factor is 3.51 and the wavelet is called low-Q Morlet [9]. The $\Psi(f)$ is still a bandpass filter however it has fewer oscillations and the relative bandwidth is more; in this case it is 0.28 in comparison to 0.049 for the case of high-Q Morlet.

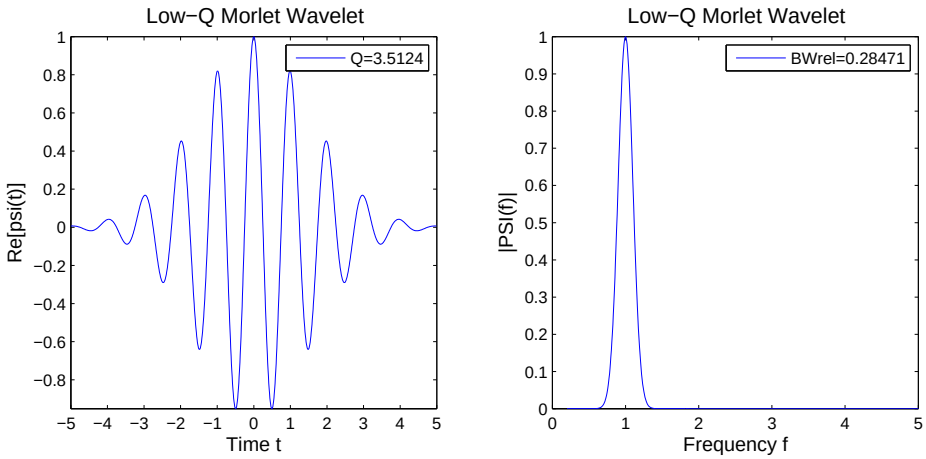

Figure 3.9: Low-Q Morlet in time domain (left hand side) with time unite t, and frequency domain (right hand side).

3.3.2 Fixed Bandwidth Filters

The filter banks were stored on the hard disk of the computer so that they could be used several times in order to compare results using different parameters to create filter banks. Tests have been done (see 4.3) on simulated signals with $10dB$ SNR to find proper value for the bandwidth. The reason to chose this amount of noise to add to the simulated signal is that the color tone of *BackGroundArea* in this case, resembles the color tone of *BackGroundArea* of most of the clinical signals available in this study. In these tests, bandwidths between 0.02 and 0.2 were examined. Due to the characteristics of the wavelet, using a value smaller than 0.02 was not possible and for values above 0.2 there were not any considerable improvement so that these values were decided as the limits.

A MATLAB code was implemented to create fixed bandwidth filters. This code calls another code to create $\psi(t)$ function to be used to create filters and then stores them. The code receives various parameters as input and stores the filters in a given destination on the hard disk. These values include the sampling frequency of the clinical (or simulated) signal to been analyzed, increment steps in the scene of frequencies, sampling frequency of the $\psi(t)$, and parameters to create the $\psi(t)$, and finally a destination to store the filters. The length of the signal to be analyzed is inputted to the code so that the created filters match signal(s) lengthwise. Frequencies to be analyzed have to be between a value in the low

frequency region and half of the sampling frequency of the signal to be analyzed.

3.3.3 Varying Bandwidth Filters

Another MATLAB code was implemented to create and store varying bandwidth filters. This code receives desired relative bandwidth, *c*, vector of scales, length of clinical (or simulated) signal to been analyzed, and destination directory on the hard disk. Likewise the other code, this code also calls the code to create $\psi(t)$ function. Vector of scales is basically a conversion between the vector of frequencies to be analyzed and scales in the time-scale representation that is resultant from the wavelet transform. This vector is created based on the sampling frequency of the signal to be analyzed, sampling frequency of the $\psi(t)$ function, and the vector of frequencies (see equations 2.20 and 2.21).

Chapter 4

Results

4.1 Analyzing the Noise Content of Clinical Data

Applying the definition of the *CancellationLevel* (see 3.2.2.2) to the different clinical signals available in this study we may observe that *CancellationLevel* may vary from infinitesimal values like 1% up to high values like 25%. The reasoning of this diverse range is based on the level of the values of the *BackGroundArea* in comparison to the pure signal. Choosing a value up to 25% would result in an acceptable definition of the mean frequency waveform while affecting (reduction) values of the pure signal the least. Deciding for values greater than 25% would manipulate the main features of the signal in a way that the result may be altered and lead to a fallacious mean frequency waveform. Needless to mention that for clinical signals with a better definition (bigger difference between the values of the *BackGroundArea* and the signal in the matrix *Pcalculated*) it is feasible to use a smaller value for the *CancellationLevel*. Speaking in the sense of the spectrogram of a signal, such as the one in figure 3.2, a clinical signal with a better definition means that the color tone of its *BackGroundArea* is more of a bluer color and the color tone of the signal itself is more redder. Thus a clinical signal with the worst situation is the one that has a smaller difference in the color tone of the two areas. To give an example of such a case, we can compare the results previously represented in figure 3.7 with figure 4.2. In this figure we can see that despite the high *CancellationLevel*, 18% (in comparison to 3.4% for the case of figure 3.7),

we still have small, but effective, presence of the *BackGroundArea* after the noise reduction process.

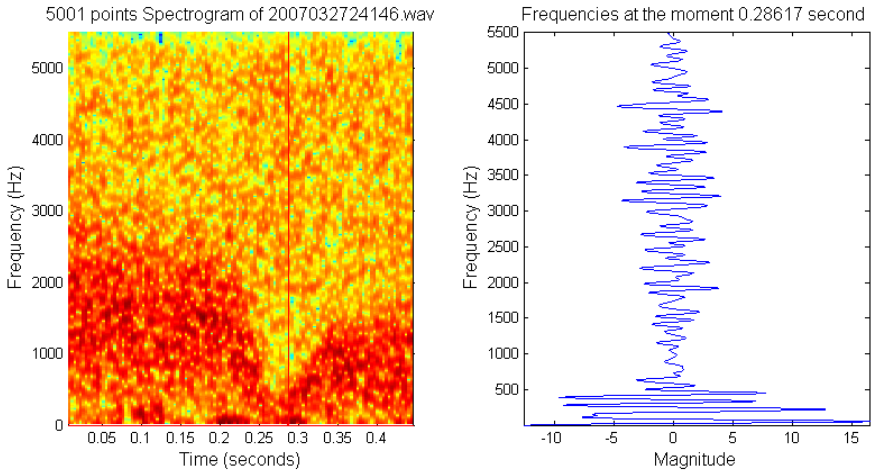

Figure 4.1: Spectrogram of a portion of a clinical signal (right hand side) in which an arbitrary instant of time (0.286 second) is marked with a red vertical line and magnitude of frequency variations (left hand side) at that instant of time.

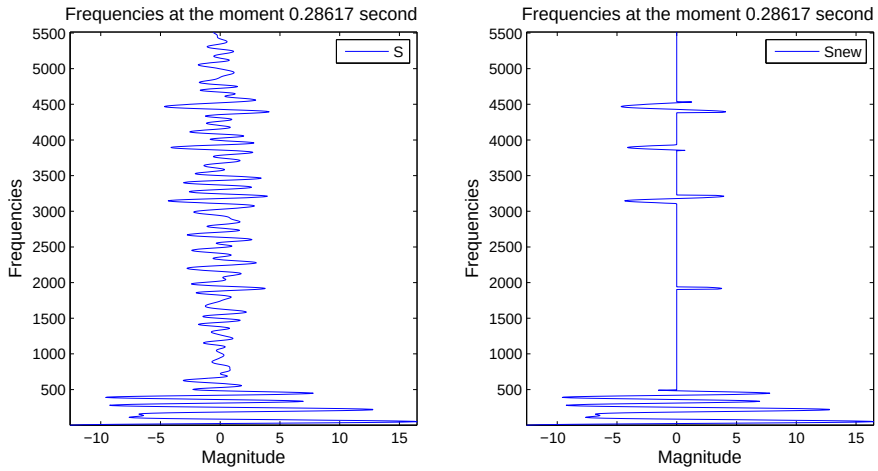

Figure 4.2: Comparison of magnitude of variations of frequency at the time instance of right hand side plot of 4.1 before (left) and after noise reduction (right).

Note that in the case of this instant of time, the main values of frequencies of the signal are in a frequency range inferior to $500Hz$. However, analyzing the plot on right hand side of figure 4.1, one can notice the presence of strong spikes (around 3200, 4000, and 4500 Hz) which prevailed the previously applied noise

reduction process. Due to the multiplication of the values of powers at each instant of time-frequency with the value of the frequency bin (see equation 2.28), the existence of a few spikes in the higher frequency region in the *BackGroundArea* would dramatically affect the mean frequency calculation.

In the figures 4.3 to 4.5, we have tested 3 different clinical signals. In each figure there are 3 sub plots. The one on top represents the spectrogram of a portion of a clinical signal, the middle one is the result of application of the noise reduction technique to the clinical signal using *CancellationLevel* of 1%. This means that the root mean square (RMS) of the matrix $SnoInfo$ is directly used as the $Threshold$ value ($Tolerance = 1$). Finally the bottom graph shows the smallest possible *CancellationLevel* that leads to an acceptable mean frequency waveform estimation. By an acceptable estimation of the mean frequency waveform we mean an estimation that by looking at it, one could relate different features of the waveform to the spectrogram of the clinical signal. That is an estimation that would follow the variations of frequency the best. It is possible to relate the color tone of the *BackGroundArea* and the magnitude of the difference between color tone of two areas with a required amount of $Threshold$ (or in another sense $Pthreshold$. To appreciate this relation, we can compare the $Pthreshold$ in these three figures. From this comparison, it can be concluded that a more reddish background requires a higher $Pthreshold$. In these particular cases $Pthreshold$s of 5.84×10^{-8}, 1.04×10^{-6}, and 5.83×10^{-6} are sufficient to obtain acceptable results from these particular clinical signals. The mentioned $Pthreshold$s correspond to 2%, 21% and 27% of *CancellationLevel*, respectively.

Fine tuning of the parameters required for the noise reduction procedure enabled the calculation of the mean frequency waveform (as mentioned in literature, i.e. [5]) with high accuracy level. However it is worth to mention that due to clinical nature of some of them there are examples that portions of the audio files are severely affected by high levels of noise in such a way that no waveform could be extracted from them whatsoever. This could be intuitively understood by simply listening to their corresponding audio file. Considering the spectrogram of such cases, we can see that for time instants that the signal is acutely

battered, we have presence of values not only in the low frequency region, but rather the whole frequency scope. This is seen as both thick and thin reddish columns covering most of the frequency scope along the spectrogram. Clinical signal 2007032219143.*wav* is an example of such a case.

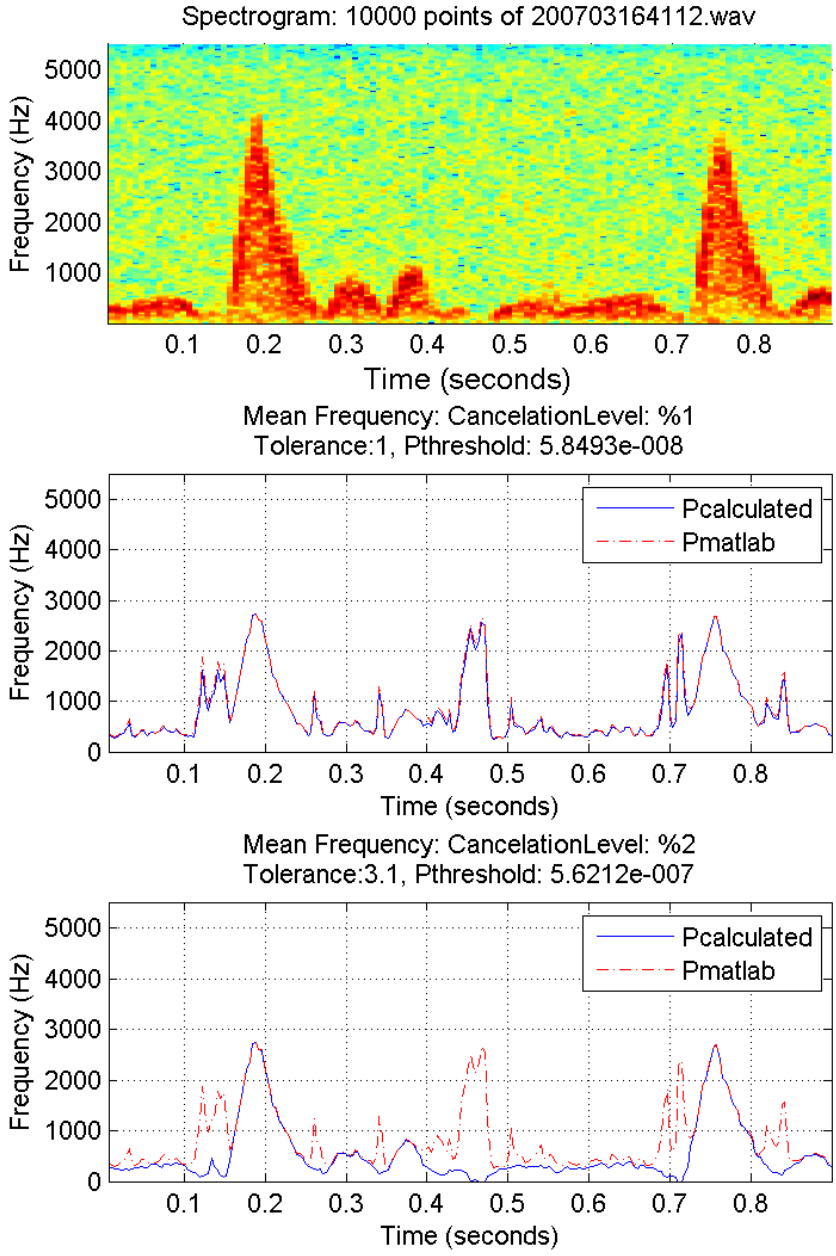

Figure 4.3: Spectrogram of a portion of a clinical signal (top), center frequency estimation without noise cancellation (middle) and with noise cancellation (bottom) with *Pthreshold* of 5.62×10^{-7}.

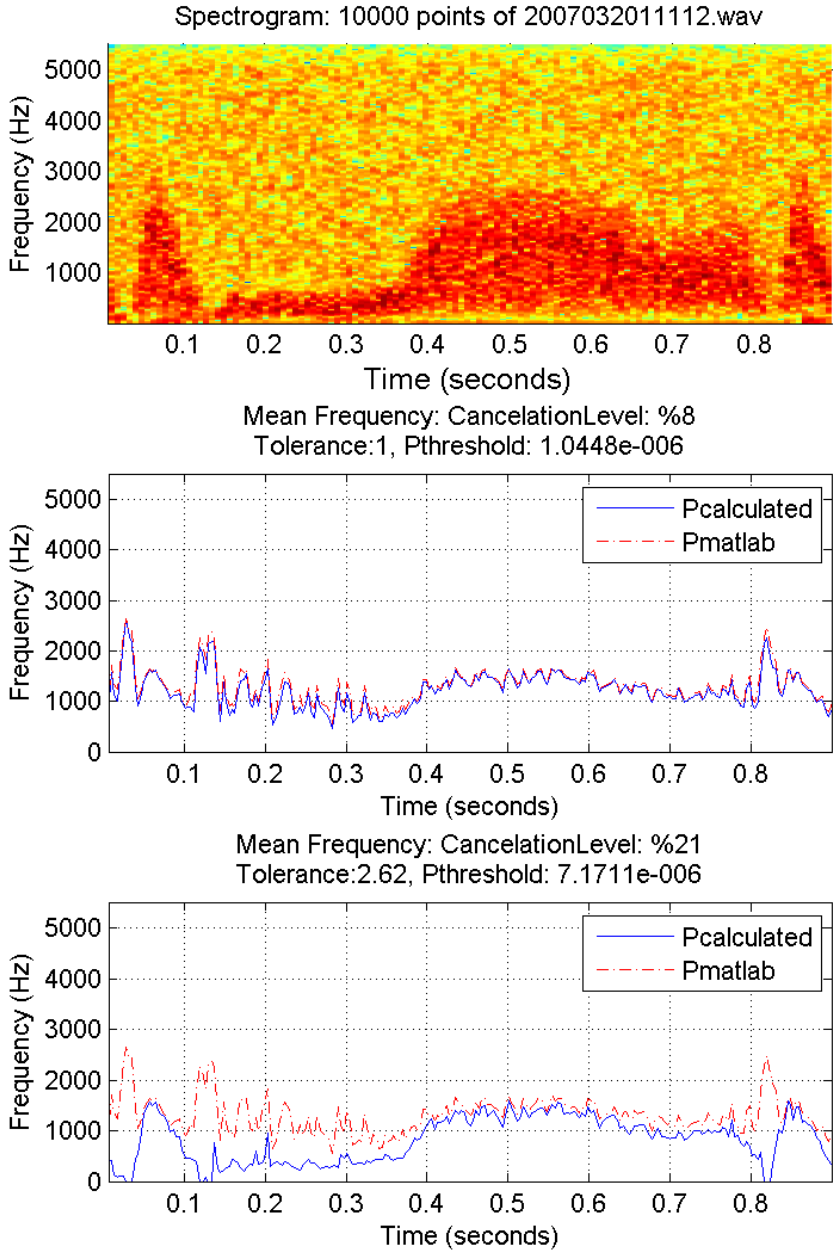

Figure 4.4: Spectrogram of a portion of a clinical signal (top), center frequency estimation without noise cancellation (middle) and with noise cancellation (bottom) with *Pthreshold* of 7.17×10^{-6}.

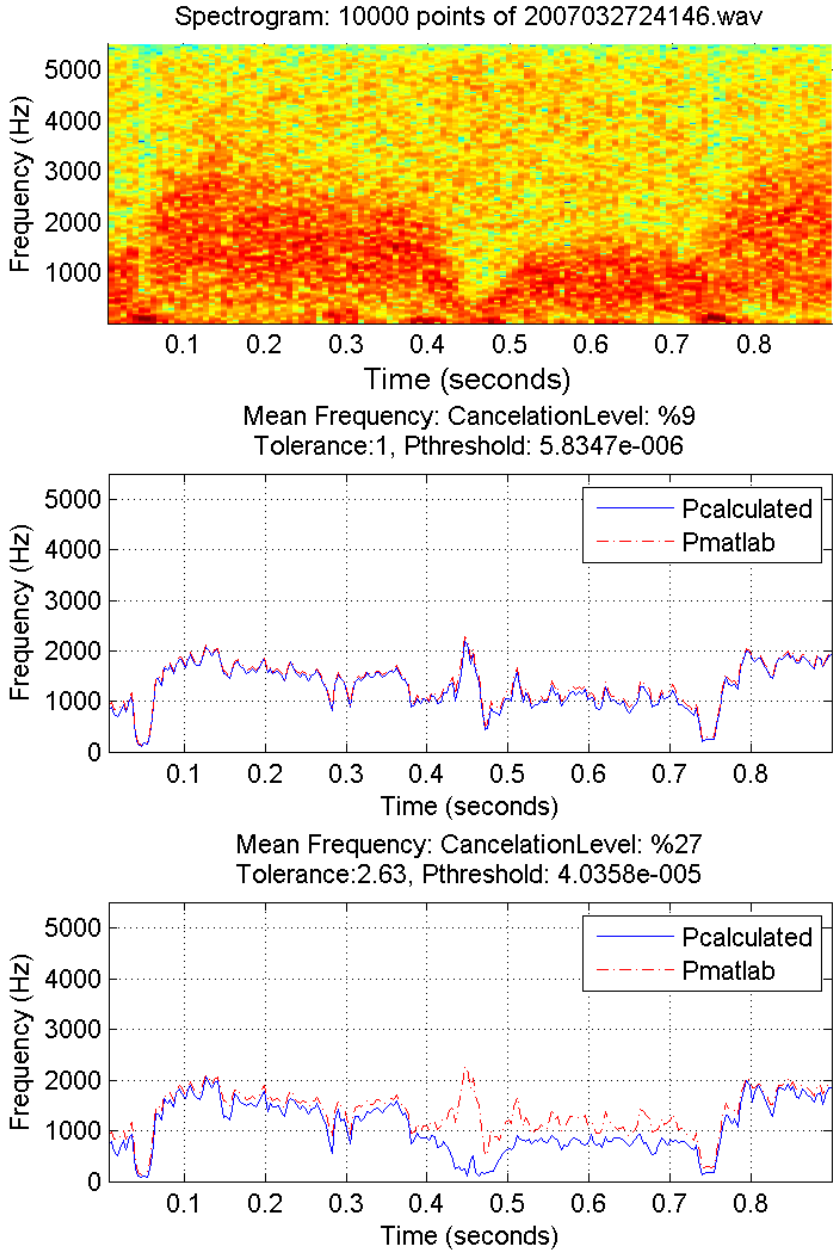

Figure 4.5: Spectrogram of a portion of a clinical signal (top), center frequency estimation without noise cancellation (middle) and with noise cancellation (bottom) with *Pthreshold* of 4.03×10^{-5}.

4.2 STFT on the simulated signal

To appreciate the performance of implemented noise reduction technique, STFT was applied on simulated signals enhancing the technique. Then results were compared against the deterministic center frequency used in the process of simulation. The comparison gives an image that how accurate is the estimation.

Center frequency of hundred simulated signals were obtained by using STFT and were averaged. Then bias of the result was calculated as the absolute value of the difference between the value of the deterministic center frequency and the estimated center frequency at each time instant. Figure 4.6 represents the deterministic center frequency curve (right hand axis) against the bias curve (left hand axis) between the 100 averaged mean frequency curves and the deterministic one while STFT with noise reduction technique was employed. As a reference the zero line is traced in the graph. Figure 4.7 corresponds to the bandwidth estimation of these 100 mean frequencies.

Concerning the performance of different methods of spectral estimators, it was observed that their accuracy is different for different features of identical simulated signals. To be more precise, it was seen that one method could follow steep changes in the frequencies (high frequencies with short duration in time) within the center frequency curve more accurately; while another one could estimate the curve more precisely when the frequency level is rather constant as low frequency and long duration in time (compare figures 4.6, 4.9 and 4.11). Therefore the deterministic center frequency curve (as well as the results of estimations) was segmented into 3 regions: Mountain, Valley and Steppe.

Mountain as the big hill-form in the first half of the waveform. Mountain segment demonstrates a huge frequency sweep and covers a range of frequencies approximately between $1000Hz$ and $4500Hz$. On a time-slice of almost 0.2 seconds, there is an uphill and a downhill. Valley segment has a small decrease and a following increase in frequency, approximately in the middle of the waveform. Finally the rest of the waveform, where the values are in a vicinity of $1000Hz$ was

named Steppe. In figure 4.6 Mountain and Valley regions are indicated by text above arrows. An ideal estimator is the one that could follow the huge and small frequency changes in the Mountain and Valley region, as well as maintaining a good approximation of the Steppe region as relatively the flat part of the waveform.

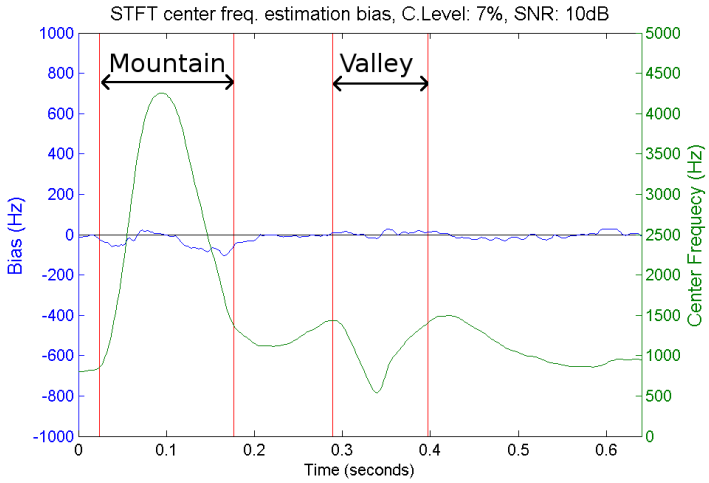

Figure 4.6: Bias of the center frequency estimation (left hand axis) using the STFT and noise reduction technique with CancellationLevel of 7%, plotted against the deterministic center frequency curve (right hand axis).

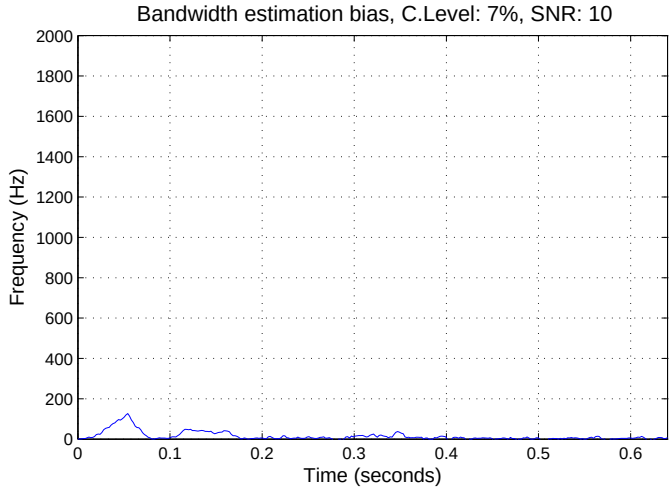

Figure 4.7: Bias of bandwidth estimation using STFT.

If the simulated signal represents a 640 millisecond segment of a cardiac cycle, on the deterministic center frequency curve, the peak of the Mountain takes place at 95 millisecond. Regarding the peak of the Mountain, the Mountain region is between 25 and 177 millisecond; the bottom of Valley is taking place at 333 millisecond and regarding this point, the Valley is between 290 and 395 milliseconds. The rest belongs to the Steppe region. These values were chosen empirically. Segmenting resultant averaged center frequency estimations was done regarding the relation of position (in time) of these points with the instants of time in which maximum and minimum occur in the Mountain and the Valley region. In figure 4.6 these time instants are represented with vertical red lines.

In table 4.1 we can see the values of maximum, minimum and average of the bias at each region in the top row when the center frequency was estimated using STFT. Window length of 15.7 millisecond and overlap of 13.75 millisecond (87%) was used. The Spectrogram function was employed with 128 frequency bins. In this study 3 different levels of SNR for simulated signals were investigated [16]. The signal to noise ratio of the analyzed simulated signals in this example was $10dB$ and noise $CancelationLevel$ of 7% was applied.

4.3 Fixed Bandwidth Filter on the Simulated Signal

In order to choose a bandwidth for fixed bandwidth filters, tests have been done and different parameters were tested. Values of maximum, minimum and average were obtained for each 3 regions.

By testing bandwidths of 0.03, 0.05, 0.07, 0.09, 0.11, 0.13, 0.15, 0.17 and 0.19, we have observed that it is not possible to determine a specific single pattern in the values of the bias to identify the best option. Nevertheless, as different bandwidths performed better for different segments and different parameters, it is recommended to define the criteria of selection based on the requirement of a particular application.

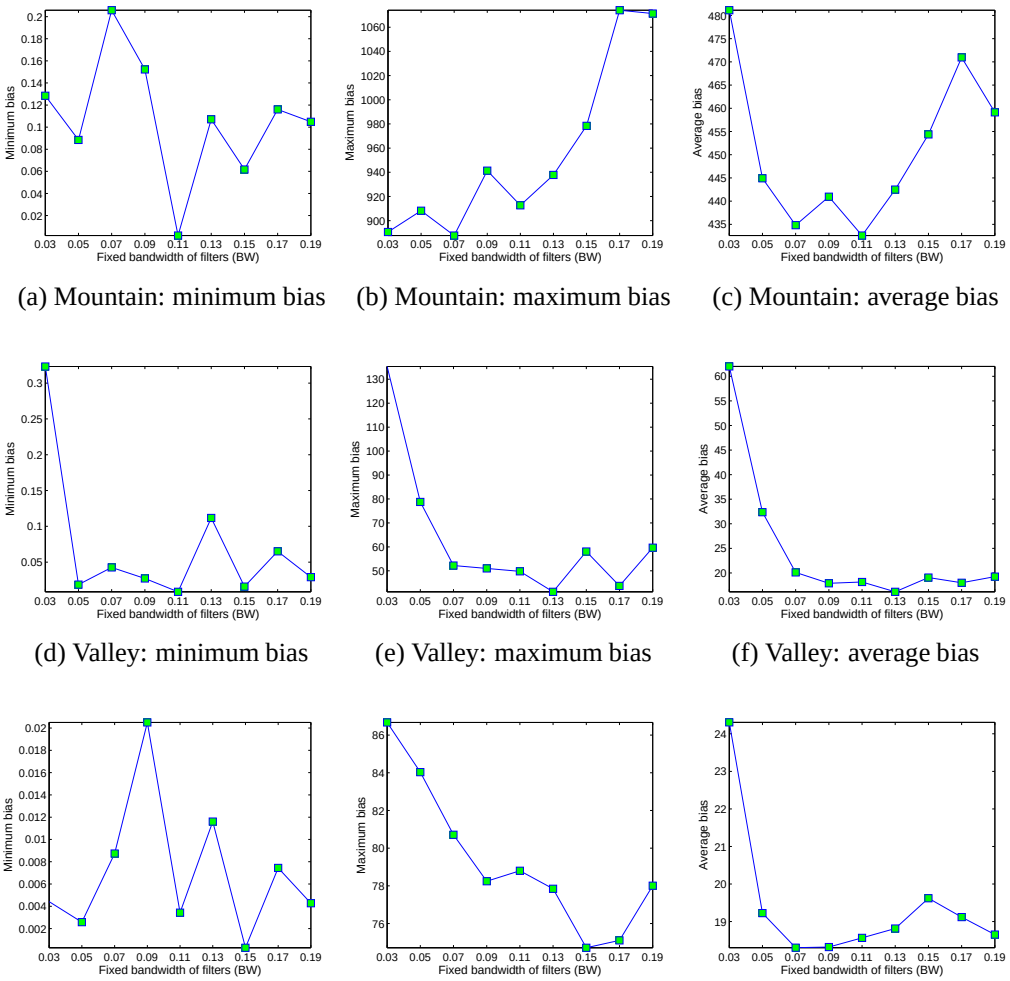

(a) Mountain: minimum bias (b) Mountain: maximum bias (c) Mountain: average bias

(d) Valley: minimum bias (e) Valley: maximum bias (f) Valley: average bias

(g) Steppe: minimum bias (h) Steppe: maximum bias (i) Steppe: average bias

Figure 4.8: Bias of mean frequency estimated curves at three regions when 9 different bandwidths of 0.03, 0.05, 0.07, 0.09, 0.11, 0.13, 0.15, 0.17 and 0.19 were employed. The values of bias in *Hz* at each bandwidth are marked with a small square.

Figure 4.8 demonstrates a graphical comparison of the performance of each of these 9 different bandwidths in the scene of value of bias in each region. The subplots in the first row correspond to the values of bias in the Mountain region, Second row is related to the Valley region and the bottom row to the Steppe region. At each row, the subplots in the left column correspond to the minimum value of the bias, the middle column is representing the maximum value of bias and the

right column exhibits the average of values of bias at each region. The horizontal axes of each of the subplots is conveying 9 points. These points correspond to each of the 9 different bandwidth in an ascending order. The vertical axes are corresponding to the magnitude of the bias. As the bias is calculated in the scene of Hertz the values on these axes are also in Hertz.

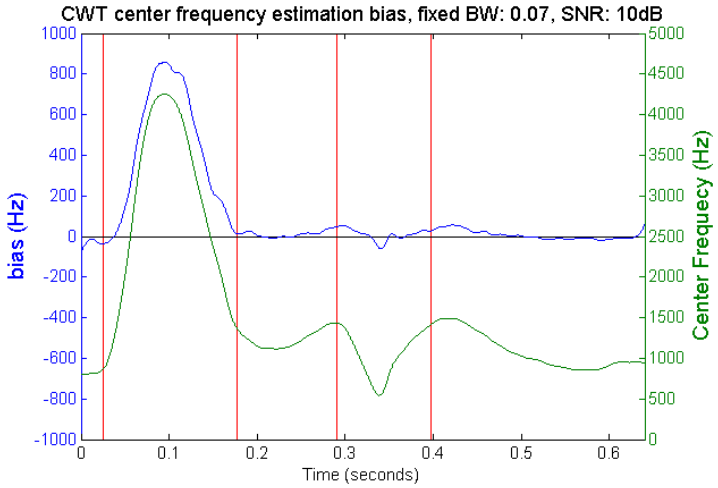

Figure 4.9: Bias of the center frequency estimation using CWT with fixed bandwidth filter of 0.07.

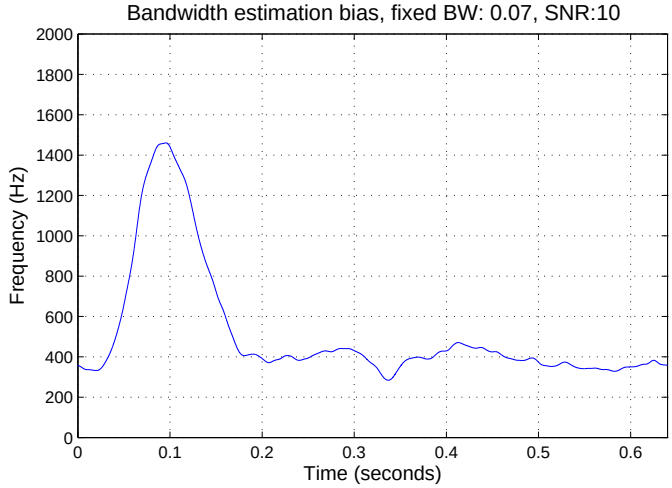

Figure 4.10: Bias of bandwidth estimation using fixed bandwidth filter.

Figures 4.9 and 4.10 are presenting the bias of estimated center frequency curve and bandwidth, respectively. The estimated center frequency curves were

averaged over 100 simulated signals and the bias (left hand axis) was obtained by subtracting it by the deterministic center frequency (right hand axis). The SNR of analyzed signals were $10dB$ and bandwidth of $0.07Hz$ was used in the process of CWT. In order to comply with the results obtained using STFT method, 128 scales were used in wavelet transformation. A scale-frequency mapping (see equation 2.20) was applied to obtain the time-frequency representation of the CWT.

4.4 Varying Bandwidth Filter on the Simulated Signal

In the table 4.1 the absolute values of maximum, minimum, and average bias of the estimated mean frequency curve are presented separately for the 3 regions. The values are obtained by employing 3 different methods: STFT with noise reduction technique, CWT with fixed bandwidth filter using 9 different values of bandwidth, and CWT with varying bandwidth filter. By comparing the values corresponding to both CWT methods, we can see that the varying bandwidth filter presents smaller maximum for the bias in the Mountain region ($280Hz$) in comparison to $912Hz$ for the best case with bandwidth of $0.11Hz$. While the STFT method presents $106Hz$ for the same region. The average of bias in the Steppe region for varying bandwidth filter is $210Hz$ which is approximately 6 times greater than the worst case of fixed bandwidth filter that is $24Hz$. For the Valley region, varying bandwidth version also presents higher averaged values than the fixed bandwidth CW version and STFT. The average of the bias in the Steppe region for the case of STFT is $13Hz$ which is relatively close to the values of the averaged bias of the Steppe region using fixed bandwidth filter. The STFT method results the least maximum and averaged bias for all the regions, however this is not the case for the minimum value of the bias.

	Mountain			Valley			Steppe		
BW	Min	Max	Ave	Min	Max	Ave	Min	Max	Ave
STFT	0.135	106	43	0.375	28	11	0.153	55	13
0.03	0.128	890	481	0.323	135	61	0.004	86	24
0.05	0.088	908	444	0.018	78	32	0.002	84	19
0.07	0.205	887	434	0.042	52	20	0.008	80	18
0.09	0.152	941	440	0.027	59	17	0.020	78	18
0.11	0.020	912	432	0.008	49	18	0.003	78	18
0.13	0.107	937	442	0.111	41	16	0.011	77	18
0.15	0.061	978	454	0.015	58	19	0.0002	74	19
0.17	0.116	1074	470	0.065	43	18	0.007	75	19
0.19	0.104	1071	459	0.029	59	19	0.004	78	18
varying	0.027	280	192	124	434	213	157	334	210

Table 4.1: Bias of estimated center frequency curve for each of the regions of observation. The top row represents the result of STFT with noise reduction technique. The 9 rows below that correspond to 9 different bandwidths for CWT with fixed bandwidth filter; the bottom line is representing the values for each region using CWT with varying bandwidth filter.

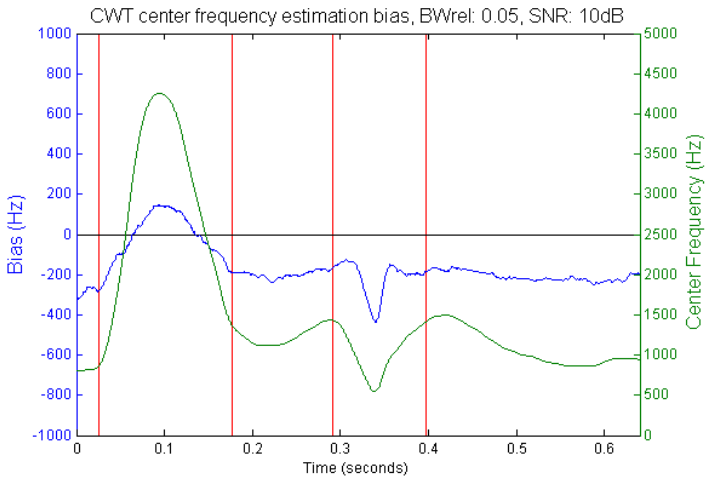

Figure 4.11: Bias of the center frequency estimation using CWT with varying bandwidth filter of 0.05.

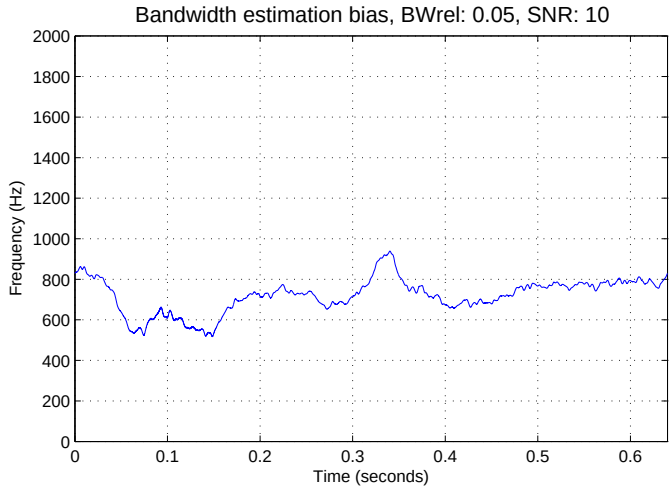

Figure 4.12: Bias of bandwidth estimation using varying bandwidth filter.

Figure 4.11 presents the deterministic center frequency curve (right hand axis) against the averaged bias of center frequency curve estimation of 100 simulated signals (left hand axis). Figure 4.12 depict the bandwidth estimation with CWT using the varying bandwidth filter. Likewise the fixed bandwidth filter, 128 scales were used in the wavelet transformation. The bandwidth of the filter used for the wavelet transformation is $0.05Hz$. The SNR of analyzed signals were $10dB$. As it is expected from the table 4.1 the estimation of center frequency in the Steppe region has a significant bias (around $-200Hz$). However this bias is rather constant and could be seen as a general offset throughout the whole waveform. The other issue to point out here is the value of the bias in the Mountain region specifically the peak of the waveform occurring roughly at $0.1ms$. This peak has a smaller bias in comparison to the one for fixed bandwidth filter (see figure 4.10). For the case of fixed bandwidth at the peak of the waveform there is nearly $800Hz$ of bias, however this value for the case of varying bandwidth is just about $200Hz$. If one assumes the bias in the Steppe region as a general offset around $-200Hz$, by elevating the bias waveform for $200Hz$ to eliminate the offset, there would be roughly $400Hz$ bias at the peak of the waveform which is still significantly less than the lowest bias in the case of fixed bandwidth filter.

4.5 Spectral Estimation of Clinical Data

In this section, the results of application of aforementioned estimators on clinical signals are presented. Three different signals with three different levels of background noise (low, middle, and high) were selected for presentation in this section. A portion of 10000 data points from each of these signals was segmented. At the end of section 4.1, the results of application of STFT on estimating the center frequency of these three signals were presented. In the current section, the same segments are being analyzed using STFT, CWT with fixed bandwidth filter and finally CWT with varying bandwidth filter to estimate center frequency and bandwidth. These results are presented in figures 4.13 to 4.15. For each signal, there are two graphs, one demonstrating the result of center frequency estimation and another one corresponding to the estimated bandwidth.

It must be mentioned that the MATLAB codes written for application of CWT (both fixed bandwidth filter and varying bandwidth filter) were modified to be used with the clinical signals. The filters used on the CWT algorithms must be designed in accordance with numerous parameters, including the sampling frequency of the input signal. The sampling frequency of the simulated and the clinical signals were $12.8KHz$ and $11.025KHz$, respectively. In contrary, the implementation of codes for the STFT is not dependent on the sampling frequency of the input signal. Therefore, the same STFT codes were used for estimating the spectral parameters of the simulated and the clinical signals.

In the graphs of the current section, STFT was enhanced by the noise reduction technique proposed in this study (see 3.2.2). In the case of each clinical signal, different amount of $Cancellation Level$ is applied. This value is mentioned in the caption of corresponding graph. In order to get a better glimpse of results of applied methods on these three clinical signals, one can compare the results with the respective spectrogram in figures 4.3 to 4.5. In these three figures, the spectrograms are presented in the top plot. In the application of STFT, window length of 14.47 milliseconds was used. The length of overlap of adjacent segments is 10.47 millisecond that corresponds to overlap of 75% of window length.

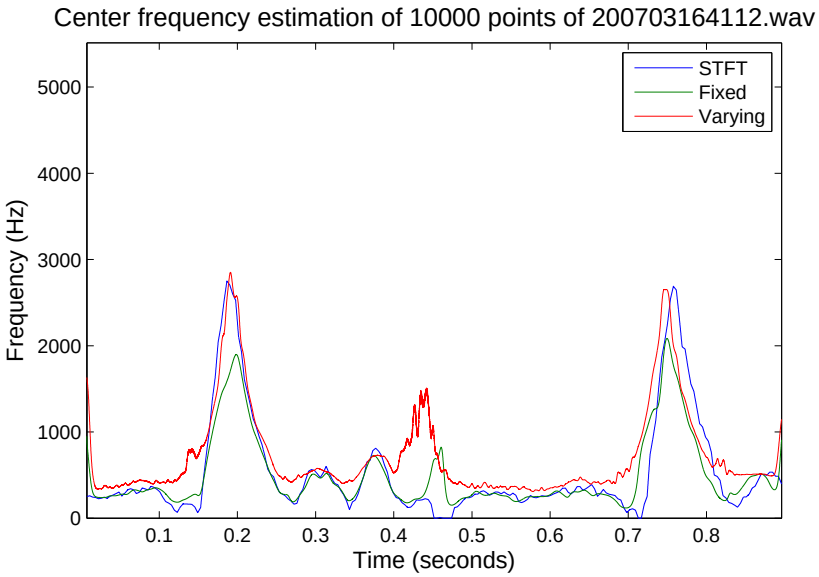

(a)

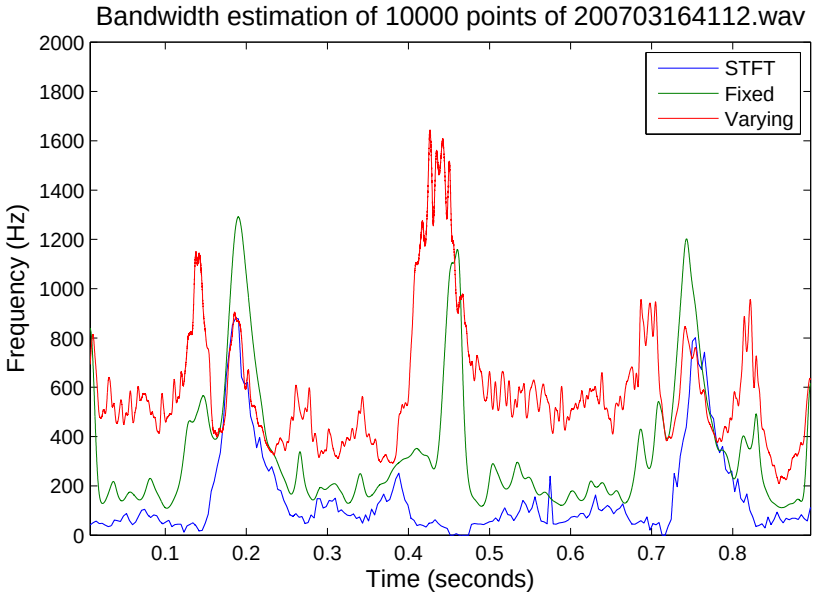

(b)

Figure 4.13: Center frequency (a) and bandwidth (b) estimation using STFT, CWT with fixed bandwidth, and CWT with varying bandwidth filter. The *CancellationLevel* in the case of STFT is 3%, *Pthreshold* is $9.36 \times 10^{-}7$ and *Tolerance* is 4.

Figure 4.13a corresponds to the clinical signal with the least noise of the three. Considering this figure, in estimating the center frequency, we can notice that all three estimators performed relatively similar in the Steppe region. In this figure one can mark the Steppe region between seconds 0 to 0.1 and 0.5 to 0.65. However the Varying bandwidth filter estimation is slightly higher than the other two. In estimating the value of peak of the Mountain, the STFT and the varying bandwidth filter performed roughly the same. The Fixed bandwidth filter estimated this value approximately 70% to 80% of the hight of the Mountain estimated with the other two methods. Varying and fixed bandwidth filters exhibited errors in Valley region (roughly between seconds 0.45 to 0.47). However it has to be mentioned that this error is overcame in the STFT due to the noise cancellation technique applied to the spectrogram of the signal. In this figure we can see that in the point of transition between the Steppe region and the Mountain region (feet of the Mountain), the STFT and Fixed bandwidth filter performed more precisely. In contrary the varying bandwidth filter suffers from overestimation at this point.

In this figure, concerning the second Mountain, one can notice a slight delay in time in the curve corresponding to the STFT estimation. The delay counts up for approximately 0.015 milliseconds.

Figure 4.13b demonstrates the bandwidth estimation of the same signal. Likewise the center frequency estimation, the fixed and varying estimators exhibit error in the Valley region. However in the bandwidth estimation this error is more acute and for the case of the varying bandwidth filter, it is extreme. The bandwidth estimation in the Valley region for the varying bandwidth filter is even higher than the peak of the Mountain. In the Mountain region, the varying bandwidth filter and the STFT estimated the value of the Mountain fairly equal. The fixed bandwidth filter estimated the value of the peak approximately 140% to 130% of the the value estimated by the STFT and varying bandwidth filter. In the Steppe region, the varying bandwidth filter estimated the bandwidth higher than the fixed bandwidth filter. The least estimation belongs to the STFT.

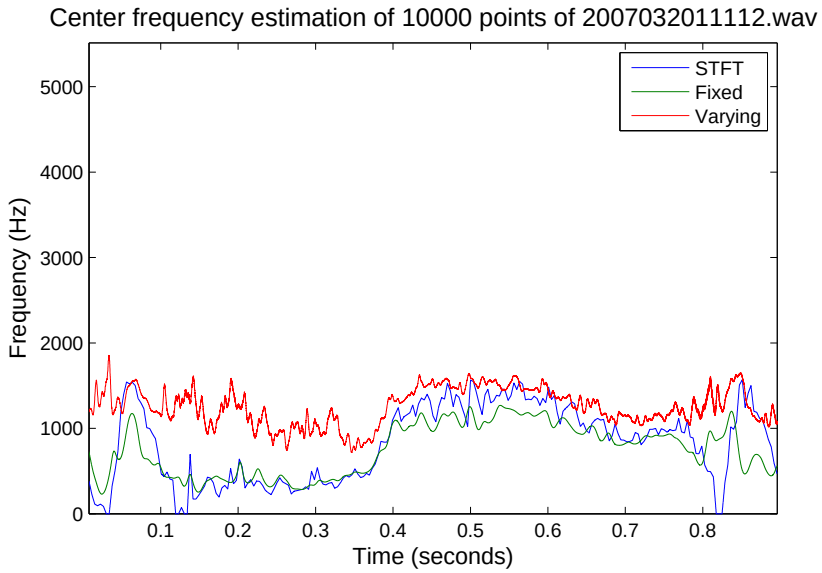

(a)

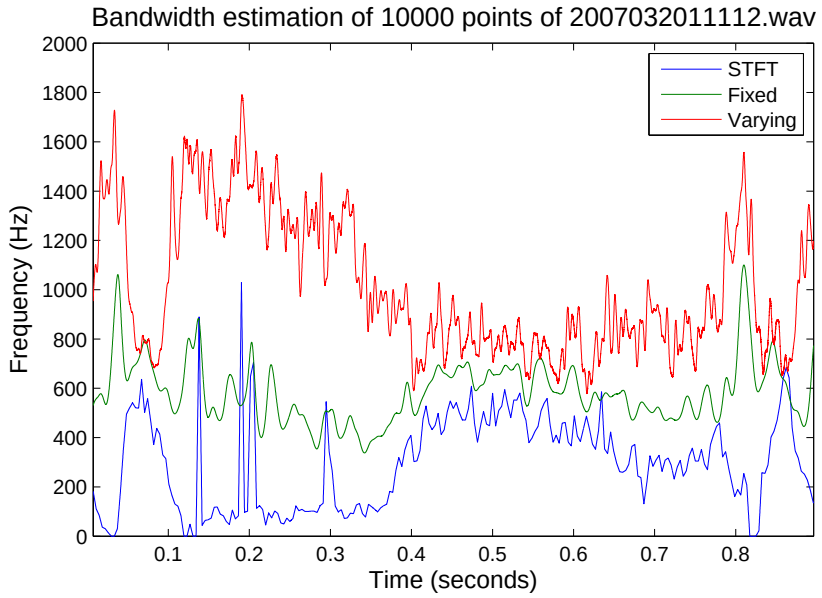

(b)

Figure 4.14: Center frequency (a) and bandwidth (b) estimation using STFT, CWT with fixed bandwidth, and CWT with varying bandwidth filter. The *CancellationLevel* in the case of STFT is 22%, *Pthreshold* is $7.86 \times 10^{-}6$ and *Tolerance* is 2.74.

In figure 4.14a one can locate the Steppe region approximately between seconds 0.15 to 0.3, and 0.45 to 0.7. In the first Steppe region, the STFT and the fixed bandwidth filter performed relatively the same. Nevertheless in the second Steppe region, that can be considered as an elevated Steppe region, the fixed filter estimated the center frequency slightly less than the STFT. In the first Steppe region the varying filter overestimated the bandwidth and in the second Steppe region (elevated Steppe) the varying filter estimated the center frequency slightly higher than the STFT. There are two Valley regions in this segment of the signal located roughly around 0.12 second and 0.82 second. The STFT method detected the Valleys at these points. On the other hand, the varying and the fixed bandwidth filter were not sensitive to the Valley region. Similar to the signal of the figure 4.13, the STFT and the varying filter estimated the peak of the Mountain fairly equal. The Mountain regions are located at 0.6 second and 0.85 second. The fixed bandwidth filter estimated these peaks slightly less than the other two.

Figure 4.14b correspond to the bandwidth estimation of the same signal. In this figure, we can notice four acute spikes in the first Steppe region in estimation of the STFT. The resultant estimated bandwidth is the least in both Steppe regions using the STFT method. In the first Steppe region, the average of bandwidth estimation of the STFT is around $100Hz$. The average for fixed bandwidth filter is around $500Hz$ and for the varying bandwidth filter it is approximately $1300Hz$. In the second Steppe region (elevated Steppe), all estimators estimated the value of the bandwidth relatively close to each other. The STFT again has the least value, and the varying bandwidth filter has the highest. The varying and the fixed bandwidth filter were not sensitive to the Valley region, however the STFT detected the Valley. In the Mountain region, the STFT has the least estimation and at the point of peak of the Mountain the varying and the fixed bandwidth filter presented roughly the same estimation. However the varying version estimated the feet of the Mountain extremely higher than the fixed one.

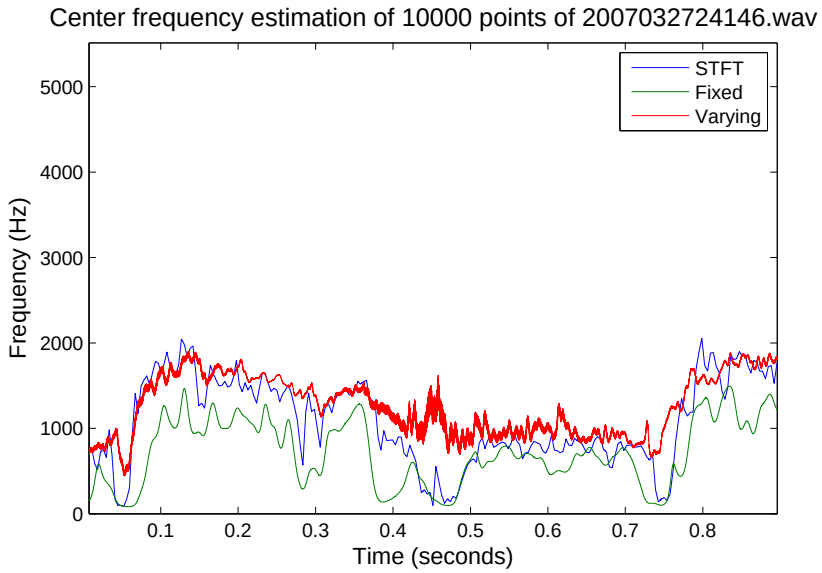

(a)

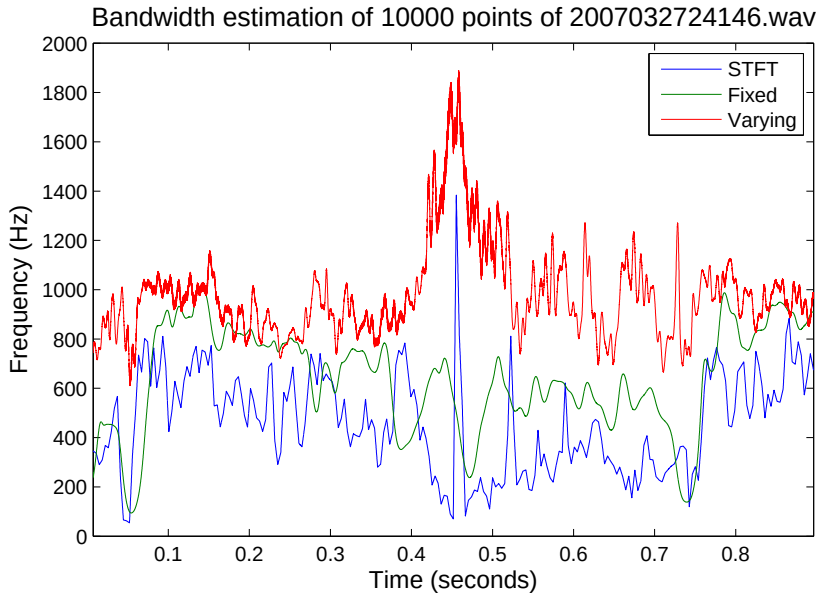

(b)

Figure 4.15: Center frequency (a) and bandwidth (b) estimation using STFT, CWT with fixed bandwidth, and CWT with varying bandwidth filter. The *CancellationLevel* in the case of STFT is 26%, *Pthreshold* is $4.04 \times 10^{-}5$ and *Tolerance* is 2.63.

The center frequency estimation of the third signal is presented in figure 4.15a. This signal has the highest BackGroundArea noise among the sample signals presented in this section. In the spectrogram of this signal that is presented in figure 4.5, one can pinpoint the two Steppe regions. Firstly between seconds 0.15 and 0.3 and the other one between seconds 0.5 and 0.7. In both Steppe regions, the fixed bandwidth filter has the least estimation and the varying bandwidth filter has the highest. The STFT and the fixed bandwidth filter exhibit relatively smoother curves, in contrary the varying bandwidth filter has fluctuations in the curve around the Valley region. The Valley region in this signal is located approximately at point 0.46 seconds. The fixed bandwidth filter estimated the value in the Valley region with a smooth concave curve. The STFT performs relatively similar but has a small spike in the bottom of the Valley. It is worth to mention that the same form of spike has been observed in the Valley region using STFT in case of an inadequate CancelationLevel selection. In this figure we can see that in spite of the high level of noise cancellation, the peak of the spike gets smaller but not omitted. On the other side, the varying bandwidth filter fails in detecting the Vally.

Figure 4.15b presents the bandwidth estimation. In this figure we can see that likewise the other two signals, the STFT has the least estimation and the varying bandwidth filter has the highest estimation. In both Steppe regions, the varying bandwidth filter failed to estimate variations in the bandwidth curve; the STFT exhibits high level of fluctuation. In the Valley region, the STFT contains a spike with a peak approximately taking place at $1400Hz$. Although the STFT and the varying bandwidth filter are two different procedures, the varying bandwidth filter formed a curve that envelops the spike detected in the Valley region.

4.6 Concluding Remarks

In the previous section the results of application of three different spectral estimators on simulated signals as well as clinical signals were demonstrated. These estimators, naming STFT with a noise reduction technique, CWT with fixed bandwidth filter and finally CWT with varying bandwidth filter were employed to es-

timate center frequency and bandwidth of signals. The simulated signals were obtained using a simulator that simulates the blood flow in the common carotid artery. This simulator is proposed by Fish et al. [5]. Three different clinical signals with different levels of background noise were selected to compare the results of these estimators.

Comparing figures 4.6, 4.9, and 4.11 one can see that STFT and fixed bandwidth filter have relatively fine approximation of the values in the Steppe region, concerning the center frequency estimation of simulated signals. Steppe region is the term proposed in this study to indicate portions of the center frequency were its value is relatively constant. Therefor one can conclude that these two methods could be used for estimation of any part of the signal were the estimated value is expected to be constant. On the other side, the varying bandwidth does not estimate satisfactorily in the Steppe region. Although the estimated value of the Steppe region using varying bandwidth filter is constant, the estimated value has a constant error of nearly $-200Hz$.

The term Mountain is proposed in this study to indicate portions of a signal where there is a rapid variation of frequency in the form of an ascending slope followed by a descending slope. Considering the simulated signals, in the Mountain region we can see that STFT performs well in estimating the value at the peak of the Mountain. However in figure 4.6 we can see that the estimators have an error of roughly $75Hz$ in both ascending and descending slopes of the Mountain. On the other hand both the other estimators behave poorer in estimating the center frequency in the Mountain region. Fixed bandwidth filter exhibits increase in the bias as the frequency increases in both slopes. The varying bandwidth filter as well has error in estimating the center frequency of the simulated signal in the Mountain region. In the particular case of the simulated signal used in this study, in the ascending slope of the Mountain, the center frequency varies from $1000Hz$ to roughly $4200Hz$. In this case, from figure 4.11 we can see that the bias of estimator varies from roughly $-200Hz$ to $+200Hz$, or in another words, $400Hz$ of increase in the estimation error is observed. Therefor we can conclude that the best choice of estimating center frequency when the frequency changes dramati-

cally in a short period of time (either increase or decrease) is the STFT with the proposed noise reduction technique. Nevertheless, the slight error of the method in steep slopes has to be considered.

In the case of Valley region, again we can confirm that STFT performs better in comparison to the other two estimators. STFT has the least error in this region. The fixed bandwidth filter estimated the center frequency better than the varying bandwidth filter. The fixed bandwidth exhibits smaller error both in the minimum point of the Valley and the descending and ascending slopes. The varying bandwidth filter has increased (absolute value) estimation error when the values of center frequency differentiate from the Steppe region.

Figure 4.7 presents the bias of bandwidth estimation using STFT. As it was mentioned in section 2.2.4 of the second chapter, the filter function used to simulate common carotid artery blood flow, has a RMS bandwidth of $100Hz$. In this figure we can verify that the STFT method using the proposed noise reduction technique, estimates the bandwidth with a good approximation (bias below $125Hz$) in most of the signal, expect the ascending slope of the Mountain region, as well as the descending slope. In the Mountain region, one can see that the bandwidth estimation has roughly $125Hz$ bias in the ascending slope and $50Hz$ in the descending slope. In the rest of the signal, we can see that the estimator performs fairly good.

Figure 4.10 presents the bandwidth estimation using fixed bandwidth filter. It can be said that the bias is basically following the center frequency curve. There is a Mountain peak with the value of approximately $1450Hz$ at the same time of the peak of the Mountain in the center frequency curve. The estimated bias demonstrate a small Valley in the same place as the Valley in the center frequency curve. In the case of the varying bandwidth filter (in figure 4.12) we can see that the bandwidth is over estimated. In this figure we can see that the values of the bias of the estimated bandwidth are around $700Hz$. It can be concluded that in the estimation of bandwidth of signals, the STFT performs the best. The fixed bandwidth filter follows the center frequency curve and the varying bandwidth filter

extremely overestimates the bandwidth.

Considering figures 4.13b to 4.15b we can conclude that the varying bandwidth filter fails to estimate the bandwidth of input signals with high level of BackGroundArea noise. This problem is more visible when the bandwidth is in the low frequency region (see figure 4.14b, first Steppe region). In the bandwidth estimation of the clinical signals, the varying bandwidth filter and the fixed bandwidth filter are not sensitive to the Valley regions. This issue is more severe for signals with high level of BackGroundArea noise. For the signals with low level of BackGroundArea noise, STFT and the varying bandwidth filter estimate the hight of the Mountain regions fairly equal; However the performance of the varying bandwidth filter is degraded in the feet of the Mountain.

Chapter 5

Conclusion and Future Work

This study was aimed to investigate the estimation of Doppler ultrasound blood flow spectral mean frequencies. Throughout the study that led to formation of this thesis, the following topics have been investigated: The Fourier analysis of Doppler blood flow signals has been studied. The MATLAB codes for calculating the STFT have been developed and explored in detail. Based on the resultant STFT the center frequency curve has been estimated. Since the goal of the study was to investigate center frequency estimation of clinical signals, the noise content of signal appeared on the STFT has been identified and isolated. Based on this representation of the noise, a noise reduction technique was proposed. This technique was basically implemented to enhance the STFT. In order to be able to evaluate the results, simulated signals with deterministic center frequency curve and added Gaussian noise were employed. In addition to STFT, Two methods of varying bandwidth filter and fixed bandwidth filter for CWT have been studied. The results of application of STFT using the proposed technique and the two methods of CWT were compared against each other. In the case of the fixed bandwidth filter, different values of bandwidth were studied and a the best bandwidth has been chosen. The decision was made based on value of the bias in different parts estimated center frequency of one cardiac cycle of the simulated signal.

Considering estimation of Center frequency in the Mountain region, it can be concluded that the STFT performs the best among the three estimators. It is

necessary to mention that in estimating the value at the peak of the Mountain, the Varying bandwidth filter estimates the value fairly close to the estimation of STFT. In the Valley region, STFT estimates the best and the performance of the fixed bandwidth filter is better than the performance of the varying bandwidth filter.

Regarding the bandwidth estimation, STFT with the proposed noise cancellation technique estimates with a satisfactory approximation in different regions. It has been observed that the varying bandwidth filter and the fixed bandwidth filter are not sensitive to the Valley region. On signals with low level of BackGroundArea noise, the estimations of value at the peak of the Mountain using the STFT and the varying bandwidth filter are fairly equal.

In the case of a *CancelationLevel* (see 3.2.2.2), it is possible to define another way to calculate this concept so that it would convey more information on the depth of the processes being applied on the signal. For instance the concept could be defined in a way to represent the distribution of the amplitudes of the matrix *Pcalculated*. So to speak it is desired to deliver some of the statistical characteristics of the power distribution in the matrix *Pcalculated*.

In the previous chapter, it was mentioned that the fixed bandwidth filter has a noticeable behavior when estimating the bandwidth. It was observed that the estimated bandwidth filter is basically following the center frequency curve (see figure 4.10). In this study, the major work was concentrated on the center frequency estimation, however these experiments and results might lead other investigators to dwell on the bandwidth estimation. Since in the case of the simulated signal, the deterministic center frequency curve is available, a researcher interested in this field can investigate a method to improve the bandwidth estimation using CWT with fixed bandwidth filter.

Another issue concerning the bandwidth estimation is occurrence of unusual spikes. These spikes are short in time and increase dramatically up to the high frequency region. Signals with high level of BackGroundArea noise, exhibit spikes

particularly in the Valley and low frequency regions. Researchers are welcomed to explore the origin of these spikes and analyze them. Nevertheless, more information on the nature of the clinical signals would be an asset in order to analyze these spikes.

Development of signal processing systems based on field programmable gate arrays or simply FPGA, is one of the progressive fields in engineering of transducers in medicine. Hu et al. [17] invested the implementation of a pulsed-wave Doppler signal processor using a FPGA based system. They have reported that usage of FPGA chips makes it possible to implement the processing unit along with the beamforming function on the same chip to enhance duplex scanning. Application of the proposed noise cancellation technique in the current study would ameliorate the performance of such digital system.

The noise reduction technique proposed in this study was basically applied on the STFT. Nevertheless, interested researchers are encouraged to investigate techniques to reduce the noise in the CWT that is the time-scale representation of signals. Due to similarity of time-scale and time-frequency representations and the fact that one can be transformed to the other one; The same technique used in STFT can be adopted for CWT. Moreover, other techniques to reduce the noise in CWT and estimate the spectral parameters more precisely would provide the means to evaluate the noise reduction technique proposed in this thesis.

Bibliography

[1] Bernard Sigel. A brief history of Doppler ultrasound in the diagnosis of peripheral vascular disease. *Ultrasound in Med & Biol*, 24(2):169–176, 1998.

[2] Graca Ruano. *Investigation of real-time spectral analysis techniques for use with pulsed ultrasound Doppler blood flow detectors*. PhD thesis, University College of North Wales, 1992.

[3] Yuanyuan Wang and Peter J. fish. Comparison of doppler signal analysis techniques for velocity waveform, turbulence and vortex measurement: A simulation study. *Ultrasound in Med & Biol*, 22(5):635–649, 1996.

[4] Xin Fang, Yuanyuan Wang, and Weiqi Wang. Doppler ultrasound signals simulation from vessels with various stenosis degree. *Ultrasonic*, 44(1):173–177, 1996.

[5] Jose C cardoso, Maria Graca Ruano, and Peter J Fish. Nonstationarity broadening reduction in pulsed Doppler spectrum measurements using time-frequency estimators. *IEEE Transactions on Biomedical Engineering*, 43(13), 1996.

[6] Leon Cohen. *TIME-FREQUENCY ANALYSIS*. Prentice Hall PTR, 1995.

[7] Larry Y. L. Mo and Richard S. C. Cobbold. ”Speckle” in continuous wave Doppler ultrasound spectra: A simulation study. *IEEE Transactions on Ultrasonics, Ferroelectrics and Frequency Control*, 33(6):747–753, 1986.

[8] Bahaa A. Saleh and Malvin Carl Teich. *Fundamentals of Photonics*, page 922. John Wiley & Sons, 1991.

[9] Carl Melvin Teich, Conor Heneghan, and Shyam M. Khanna. Analysis of cellular vibrations in the living cochlea using the continuous wavelet transform and the short-time fourier transform. In *Time-Frequency and Wavelets in Biomedical Engineering*, pages 243–269. IEEE Press, 1 edition, 1997.

[10] S ergio Matos, Ana Leiria, and M. G. Ruano. Wavelet transformation on the assessment of common carotid artery blood flow spectral parameters. In *Proceeding of World Congress on Medical Physics and biomedical Engineering*, Chicago, USA, July 2000. CD-ROM.

[11] Ana Isabel Leiria. *Spectral Analysis of Embolic Signals*. PhD thesis, Universidade do Algarve, 2005.

[12] Yuanyuan Wang and Peter J. fish. Arterial Doppler signal simulation by time domain processing. *European Journal of Ultrasound*, 3(1), 1996.

[13] Rangaraj M. Rangayyan. *Biomedical Signal Analysis, A Case-Study Approach*. John Wiley & Sons, 2002.

[14] N. Aydin and H. S. Markus. Optimization of processing parameters for the analysis and detection of embolic signals. *European Journal of Ultrasound*, 12, 2000.

[15] D. L. Jones and R. G. Baraniuk. Efficient approximation of the continuous wavelet transform. *Electronics Letts*, 27, 1991.

[16] Behrooz Zabihian, C. A. Teixeira, and M. Graca Ruano. Noise cancellation technique for Doppler ultrasound spectrogram enhancement. In *2011 Pan American Health Care Exchanges (PAHCE 2011)*, Rio de Janeiro, Brazil, March 28 - April 1, 2011. IEEE Press.

[17] C. H. Hu, Q. Zhou, and K. K. Shung. Design and implementation of high frequency ultrasound pulsed-wave doppler using fpga. *IEEE Transaction on Ultrasonic, Ferroelectrics and Frequency Control*, 55(9):2109–2111, 2008.